NATURE-BASED INFRASTRUCTURE
GLOBAL RESOURCE CENTRE

Sustainable Asset Valuation of Restoring the Mallorquín Swamp, Colombia

TECHNICAL APPENDIX

Supported by

Led by

May 2023

Published by the International Institute for Sustainable Development

The **Nature-Based Infrastructure (NBI) Global Resource Centre** aims to improve the track record of NBI to deliver infrastructure services and adapt to climate change while delivering other environmental, social, and economic benefits. We provide data, training, and customized valuations of NBI projects, based on the latest innovations in systems thinking and financial modelling.

The Centre is an initiative led by IISD, with the financial support of the Global Environment Facility (GEF) and the MAVA Foundation, in partnership with the United Nations Industrial Development Organization.

IISD
nbi.iisd.org
@iisd_sustinfra

UNIDO
unido.org
@unido

GEF
thegef.org
@theGEF

MAVA
mava-foundation.org
@MavaFdn

Sustainable Asset Valuation of Restoring the Mallorquín Swamp, Colombia: Technical Appendix

May 2023

Written by Edoardo Carlucci, Emma Cutler, Marco Guzzetti, and Morten Siersted

Photo: Luis Alveart / Flickr CC BY-NC-ND 2.0

The opinions, statistical data and estimates contained in publications are the responsibility of IISD and should not necessarily be considered as reflecting the views or bearing the endorsement of UNIDO or GEF. Although great care will be taken to maintain the accuracy of information herein, UNIDO does not assume any responsibility for consequences that may arise from the use of the material.

NATURE-BASED INFRASTRUCTURE
GLOBAL RESOURCE CENTRE

Supported by

Led by

Table of Contents

List of Figures

List of Tables

Appendix A. Causal Loop Diagram

The following figures highlight pieces of the causal loop diagram and expose the feedback loops related to environmental quality, health, income, and climate change.

Figure A1. Environmental quality feedback loops

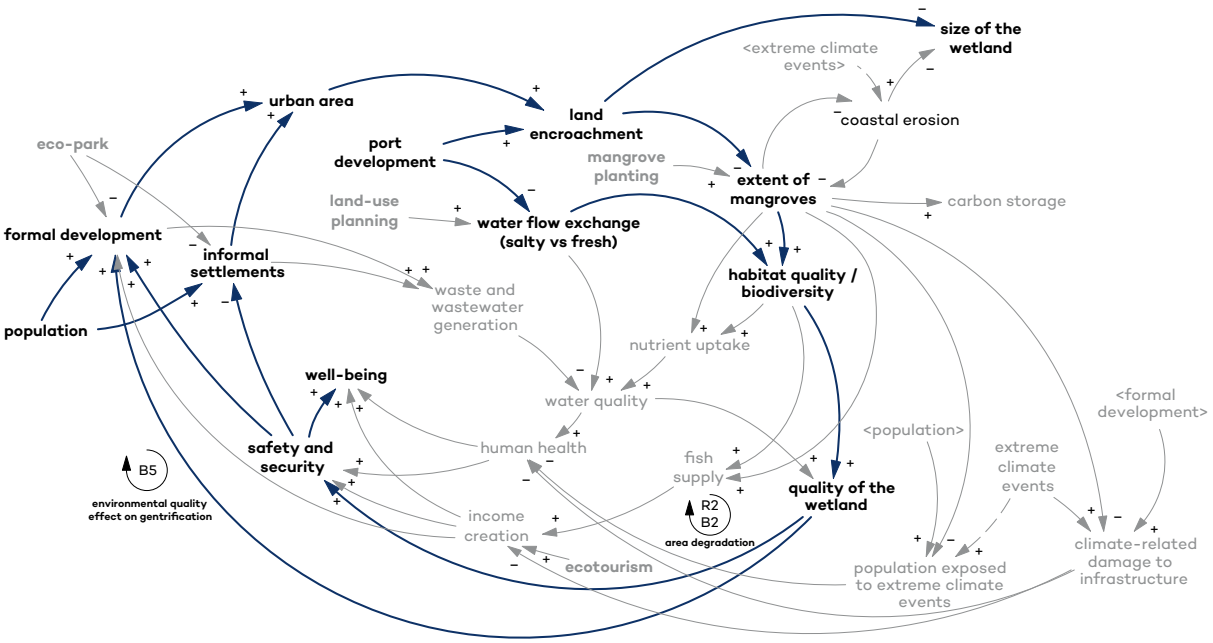

R2/B2: The declining quality of the wetland reduces safety and security, leading to more informal settlements. This further encroaches on the swamp, resulting in a smaller extent of mangroves and lower quality of the wetland. Conversely, as wetland restoration increases safety and security, there may be more formal development, restricting recovery.

B5: With a higher quality of the wetland, urbanization increases. This leads to land encroachment, which reduces the extent of mangroves and, therefore, the quality of the wetland.

Source: Authors' diagram.

Figure A2. Water quality and human health feedback loops

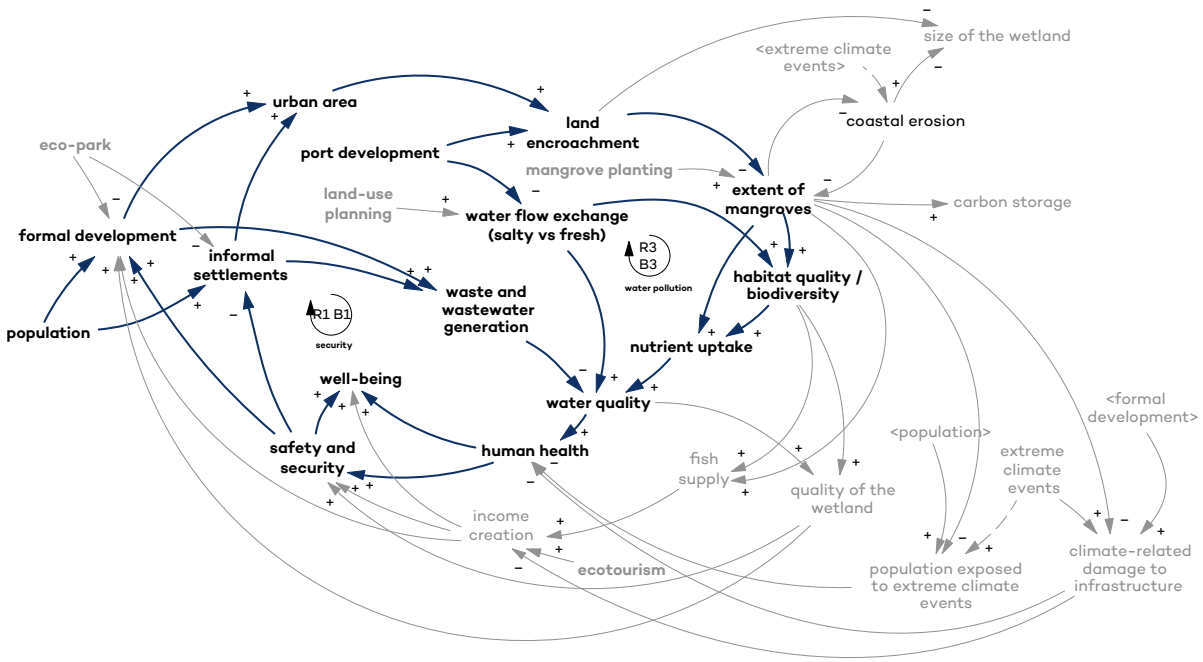

R1/B1: Urbanization leads to more waste and wastewater generation, which lowers water quality. This reduces human health and security, leading to more informal settlements and, therefore, more pollution. With improved water quality following wetland restoration, there may be an increase in formal development. This could have a negative impact on water quality but will create less pollution than informal settlements.

R3/B3:Poor water quality harms human health, which reduces security and increases informal settlements. This leads to more land encroachment, which decreases the extent of mangroves, resulting in less nutrient uptake, and therefore, lower water quality. If improved safety promotes formal development, expansion of the urban area will balance recovery of the wetland.

Source: Authors' diagram.

Figure A3. Fishing and income feedback loops

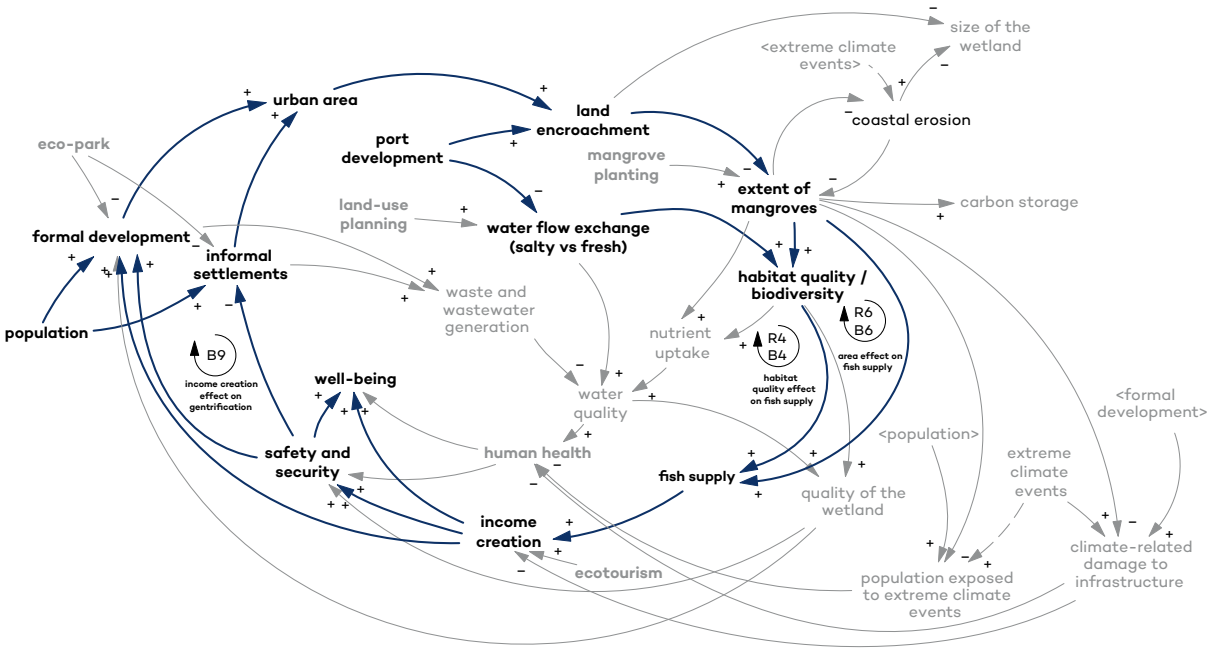

R4/B4: The loss of mangroves limits fish supply. This lowers income, creating security problems. There are thus more informal settlements, which encroach on mangroves, reducing habitat quality, further decreasing fish supply. Recovery of the fishery after mangrove restoration may attract more urbanization. There is thus a limit to how much the ecosystem will improve.

R6/B6: With a smaller area of wetland, fish supply is reduced. This decreases income, which leads to less safety and security, so there are more informal settlements. This results in more land encroachment, so the wetland area gets smaller. As with habitat quality, with more fish, formal development may increase, which could restrict the extent of mangroves.

B9: With more income from fishing and less damage from extreme events, there is more urbanization. Land encroachment thus continues. Therefore, the extent of mangroves cannot continue to increase, so the increase in fishing income and decrease in climate-related damage to infrastructure are restricted.

Source: Authors' diagram.

Figure A4. Climate change feedback loops

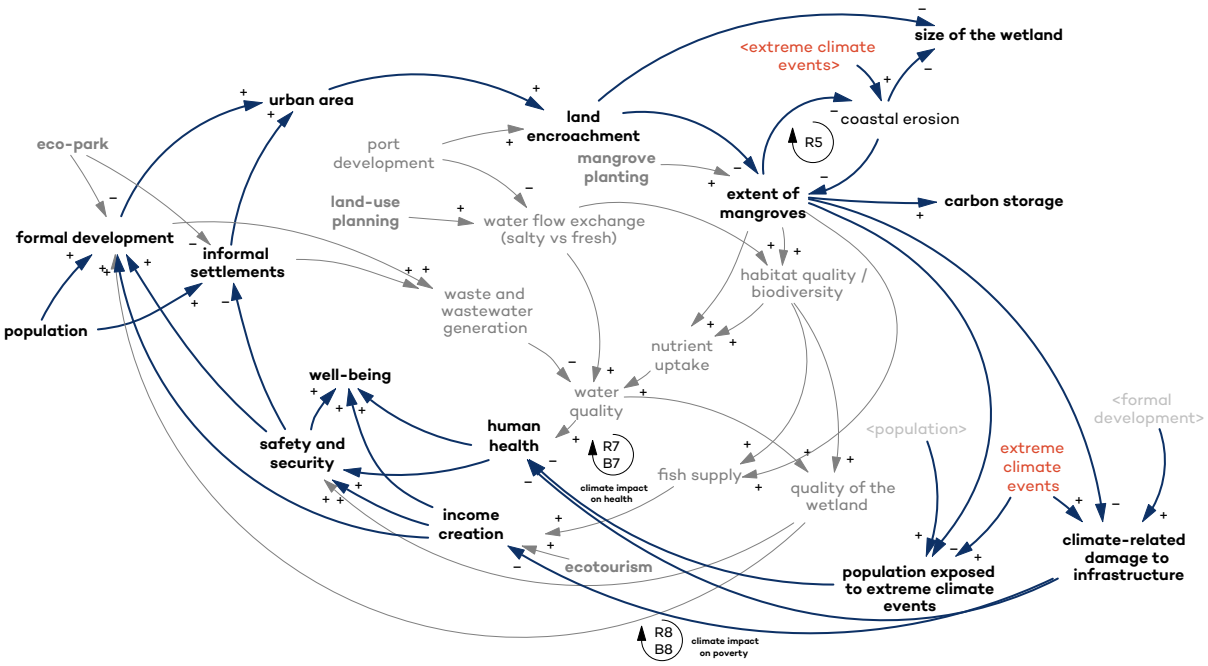

R5: The loss of mangroves increases coastal erosion, leading to a smaller extent of mangroves.

R7/B7: With more people exposed to extreme climate events and worse damage from these events, human health declines. This decreases security, so there are more informal settlements, more land encroachment, and a smaller extent of mangroves. With the loss of mangroves, exposure to and damage from extreme events increases. Conversely, as mangrove restoration decreases the health impacts of climate, there may be more urban development, limiting the area available for mangroves in the future.

R8/B8: Damage from extreme events reduces income and security. This leads to more informal settlements, so encroachment continues. This reduces the extent of mangroves, so damage increases, and income further declines. At the same time, with lower climate risk, formal urban development may limit mangrove recovery.

Source: Authors' diagram.

Figure A5. Full causal loop diagram. Feedback loops related to environmental quality, health, income, and climate change explain observed wetland degradation and loss of mangroves. Interventions (shown in orange), such as planting mangroves, conserving the area as an eco-park, land-use planning, and development of ecotourism activities, can promote environmental recovery and improve human well-being. Instead of restoring the wetland, grey infrastructure could be used to directly address the circled impacts.

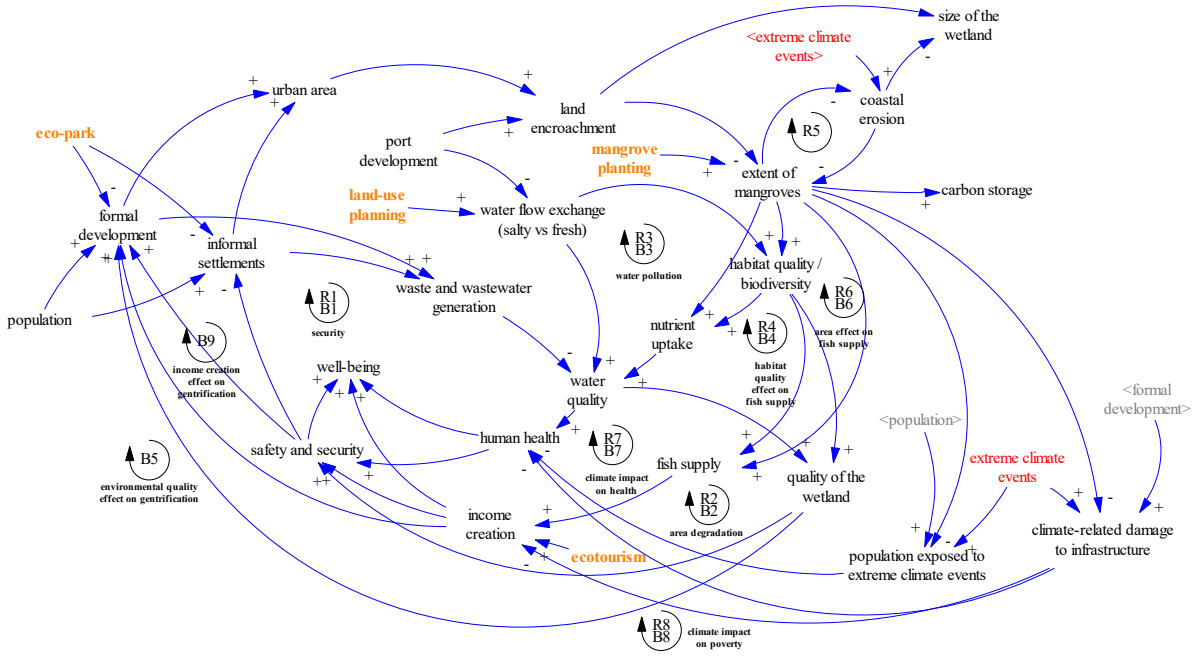

Source: Authors' diagram.

Appendix B. Spatial Analysis Report

1. Model Setup

a. Study Area

The study area of this analysis is Barranquilla, in Colombia (Figure B1).

Figure B1. Location of Barranquilla.

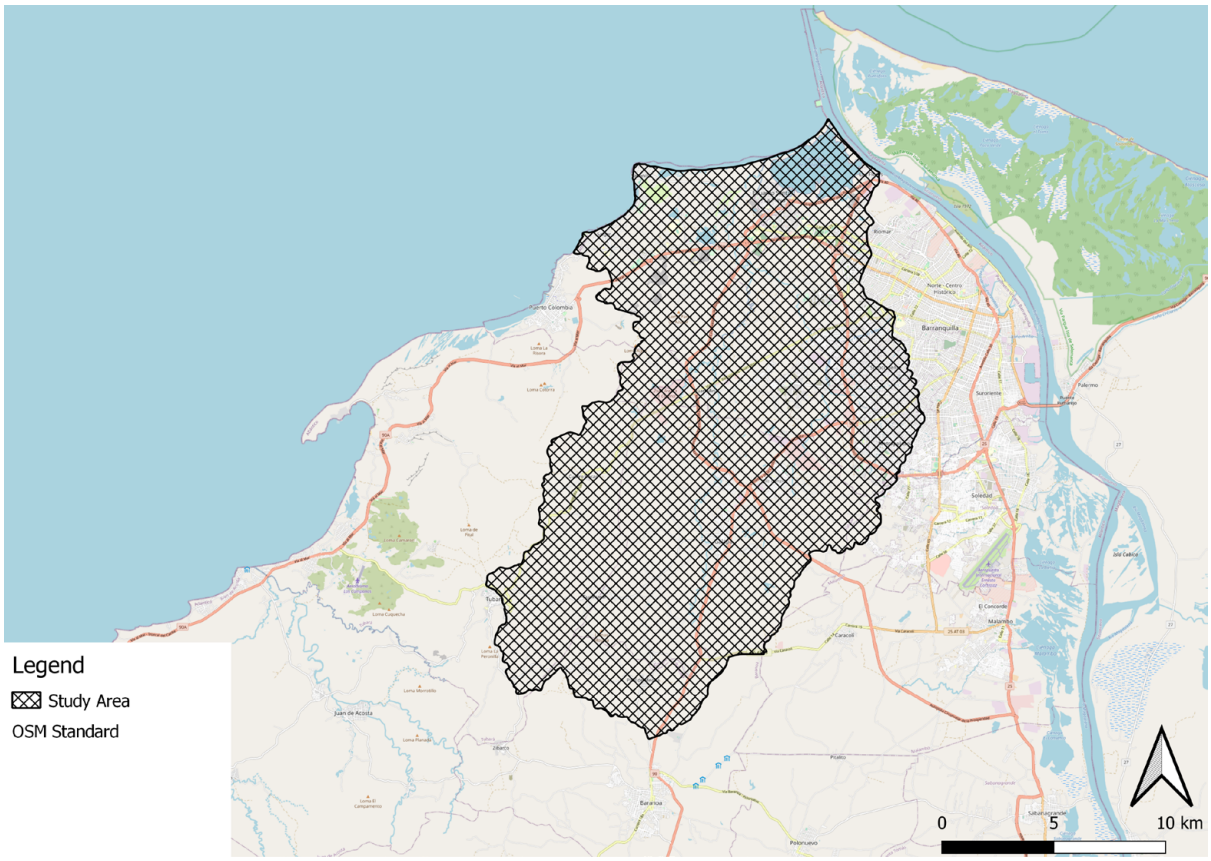

Source: Authors' diagram.

b. Coordination System

Based on world project coordinate system called "V WGS 84 / Pseudo-Mercator – Spherical Mercator – ESPG: 3857"

Here is the detailed coordinate system:

```
PROJCS["WGS 84 / Pseudo-Mercator",
  GEOGCS["WGS 84",
    DATUM["WGS_1984",
      SPHEROID["WGS 84",6378137,298.257223563,
        AUTHORITY[“EPSG”, “7030”]],
      AUTHORITY[“EPSG”,"6326"]],
    PRIMEM["Greenwich",0,
      AUTHORITY["EPSG","8901"]],
    UNIT["degree",0.0174532925199433,
      AUTHORITY["EPSG","9122"]],
    AUTHORITY["EPSG","4326"]],
  PROJECTION["Mercator_1SP"],
  PARAMETER["central_meridian",0],
  PARAMETER["scale_factor",1],
  PARAMETER["false_easting",0],
  PARAMETER["false_northing",0],
  UNIT["metre",1,
    AUTHORITY["EPSG","9001"]],
  AXIS["X",EAST],
  AXIS["Y",NORTH],
  EXTENSION["PROJ4","+proj=merc +a=6378137 +b=6378137 +lat_ts=0.0 +lon_0=0.0 +x_0=0.0 +y_0=0 +k=1.0 +units=m
+nadgrids=@null +wktext  +no_defs"],
  AUTHORITY["EPSG","3857"]]
```

c. Past Land Cover Maps

Land Cover maps downloaded from Sentinel-2 10m Land-Use/Land Cover (LULC) Timeseries Downloader (Impact Observatory for Esri, 2021) and representing the landscape of the study area as of 2017, 2019, and 2021, have been used in this assessment as shown in Figure B2, Figure B3, and Figure B4 respectively. The pixel resolution of the maps is 10 m.

Figure B2. LULC 2017

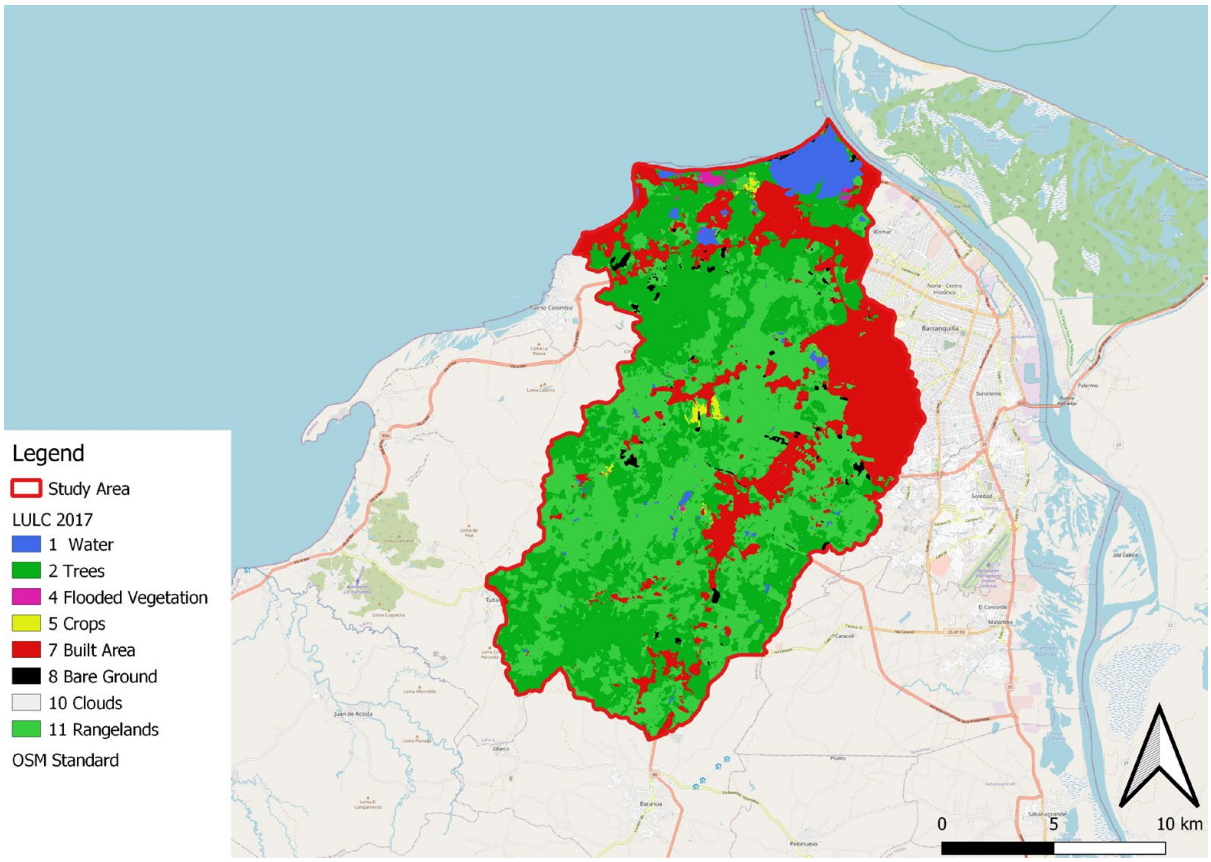

Source: Authors' diagram.

Figure B3. LULC 2019

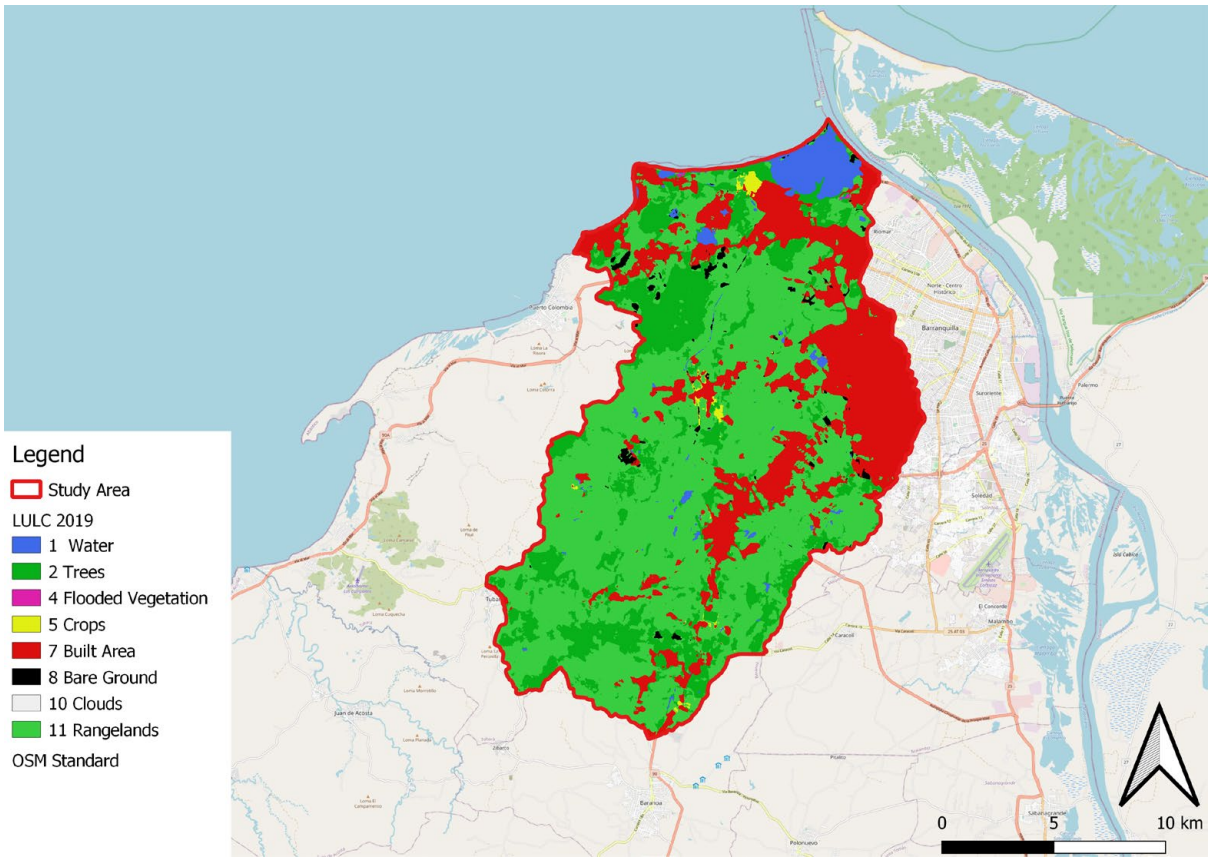

Source: Authors' diagram.

Figure B4. LULC 2021

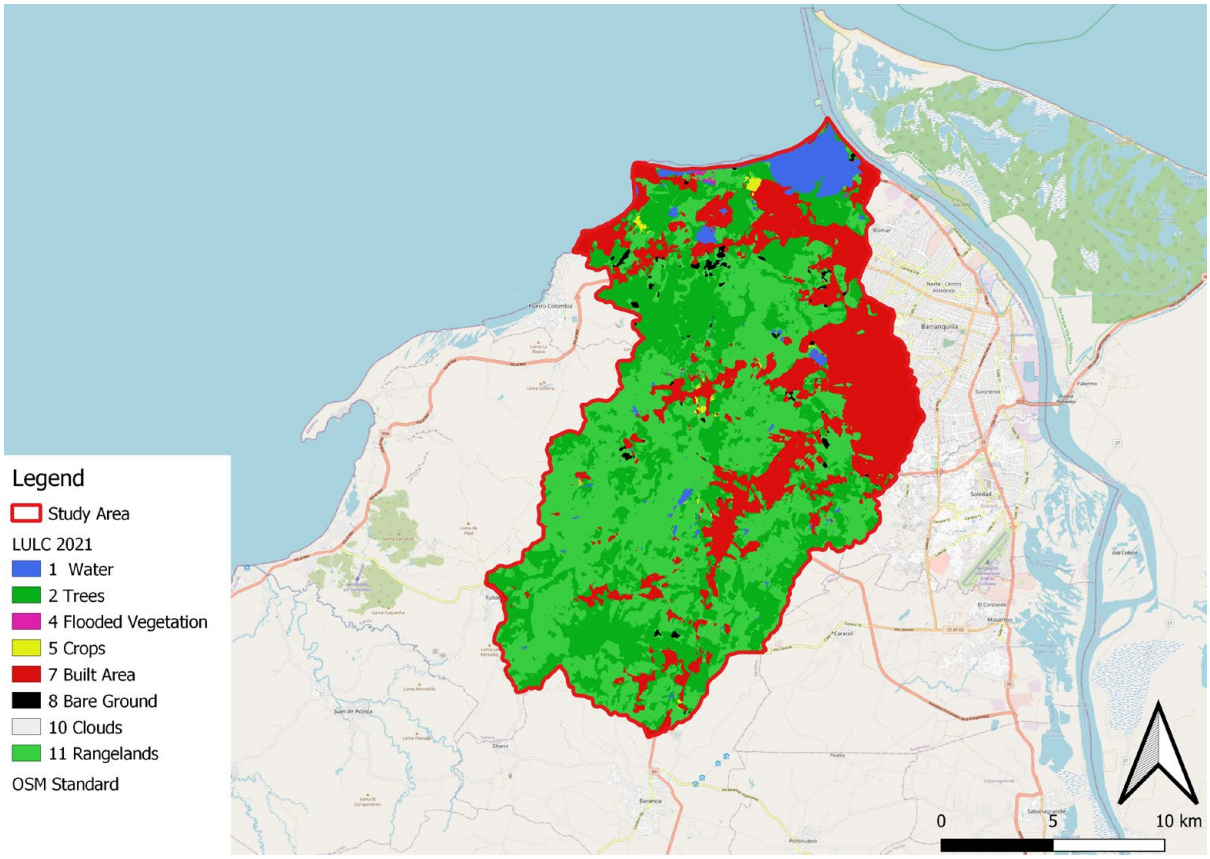

Source: Authors' diagram.

Table B1 shows the number of ha of each land class in 2017, 2019, and 2021. The table indicates that the number of ha of trees and of rangeland decreased from 2017 to 2019, and then it increased again from 2019 to 2021.

Table B1. number of ha of land classes in different years

		Number of ha		
LC number	**LC description**	**2017**	**2019**	**2021**
1	Water	1,106	1,108	1,141
2	Trees	11,416	5,555	9,298
4	Flooded vegetation	94	10	26
5	Crops	128	147	109
7	Built Area	6,302	7,059	7,305
8	Bare ground	303	312	216
9	Snow/ice	-	-	-
10	Clouds	-	-	-
11	Rangeland	11,896	17,055	13,152

d. Software and Simulation

The ecosystem services map simulation has been performed using InVEST Software V.3.9.0 (https://naturalcapitalproject.stanford.edu/invest/). The inputs spatial data for the InVEST model have been prepared by utilizing QGIS-OSGeoW-3.4.2-1 (qgis.org/downloads/). The tabulated data will be managed and prepared in MS Excel V. 2016.

2. Carbon Storage

a. Input Data Preparation and Processing

1. **LULC maps:** See Section 11.c
2. **Carbon Pools:** Table of LULC classes, containing data on carbon stored in each of the four fundamental pools for each LULC class
    - Carbon above ground: The values of carbon density in above ground mass (Mg/ha or tons/ha) of each land-use type are shown in Table B2.
    - Carbon below ground: The values of carbon density in belowground mass (Mg/ha or tons/ha) of each land-use type are shown in Table B2.
    - Carbon stored in organic matter: The values of carbon density in dead mass (Mg/ha or tons/ha) of each land-use type are shown in Table B2.
    - Carbon stored in soil: The values of carbon density in dead mass (Mg/ha or tons/ha) of each land-use type are shown in Table B2.

The unit of measurement for these coefficients is Mg/ha or tons/ha. Average carbon coefficient values have been found in the 2006 IPCC Guidelines for National Greenhouse Gas Inventories report, Chapter 4, "Agriculture, Forestry and Other Land Use" (Intergovernmental Panel on Climate Change, 2006).

Table B2. Carbon pools

lucode	LULC_ Name	C_above	C_below	C_soil	C_dead
1	lc_1	0	0	0	0
2	lc_2	141	52.17	1.36	0
4	lc_4	141	52.17	1.36	0
5	lc_5	9.87	3.6519	1.36	0
7	lc_7	0	0	0	0
8	lc_8	0	0	0	0
9	lc_9	0	0	0	0
10	lc_10	9.87	3.6519	1.36	0
11	lc_11	37.6	13.912	1.36	0

b. Results

Figure B5, Figure B6, and Figure B7 show the amount of carbon stored, in Mg, in each pixel using the LULC 2017, LULC 2019, and LULC 2021 respectively. They are a sum of all the carbon pools provided by the biophysical table.

Figure B5. Carbon model outputs (LULC 2017).

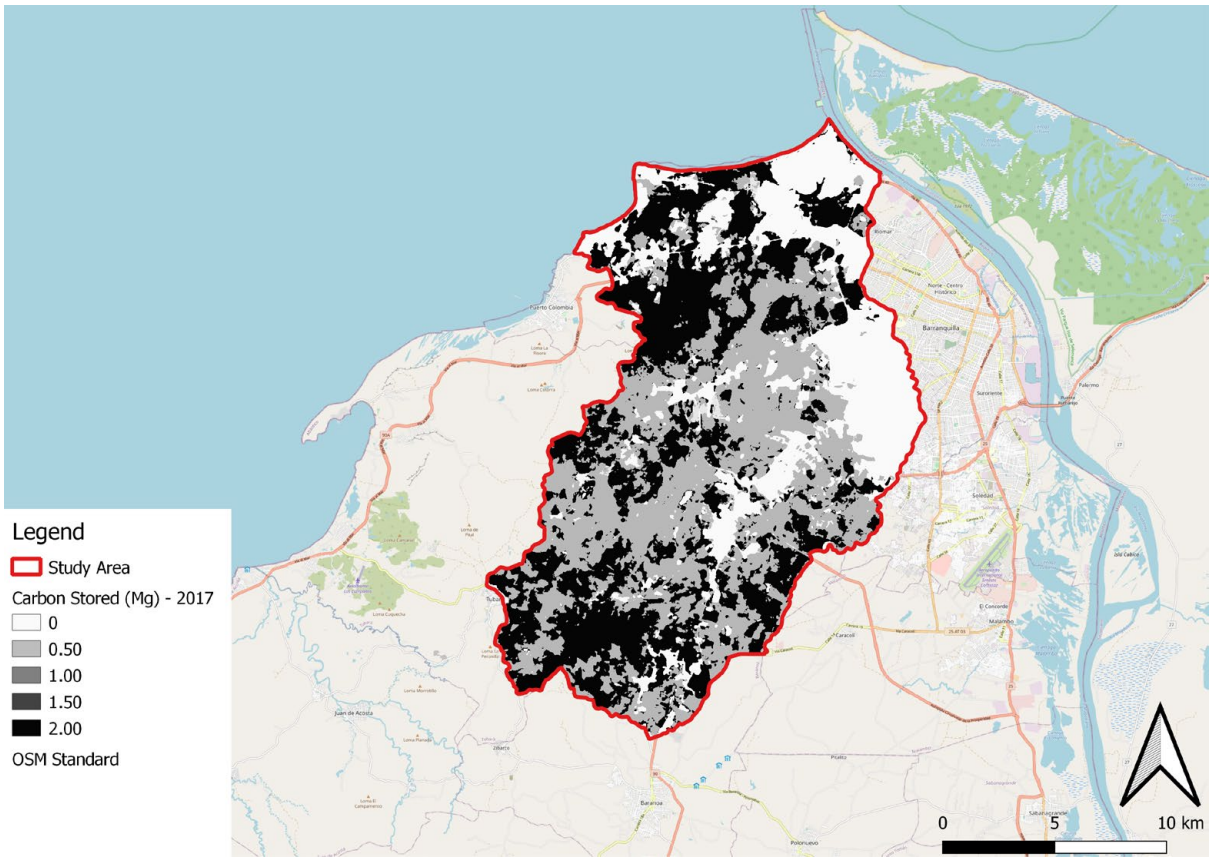

Source: Authors' diagram.

Figure B6. Carbon model outputs (LULC 2019).

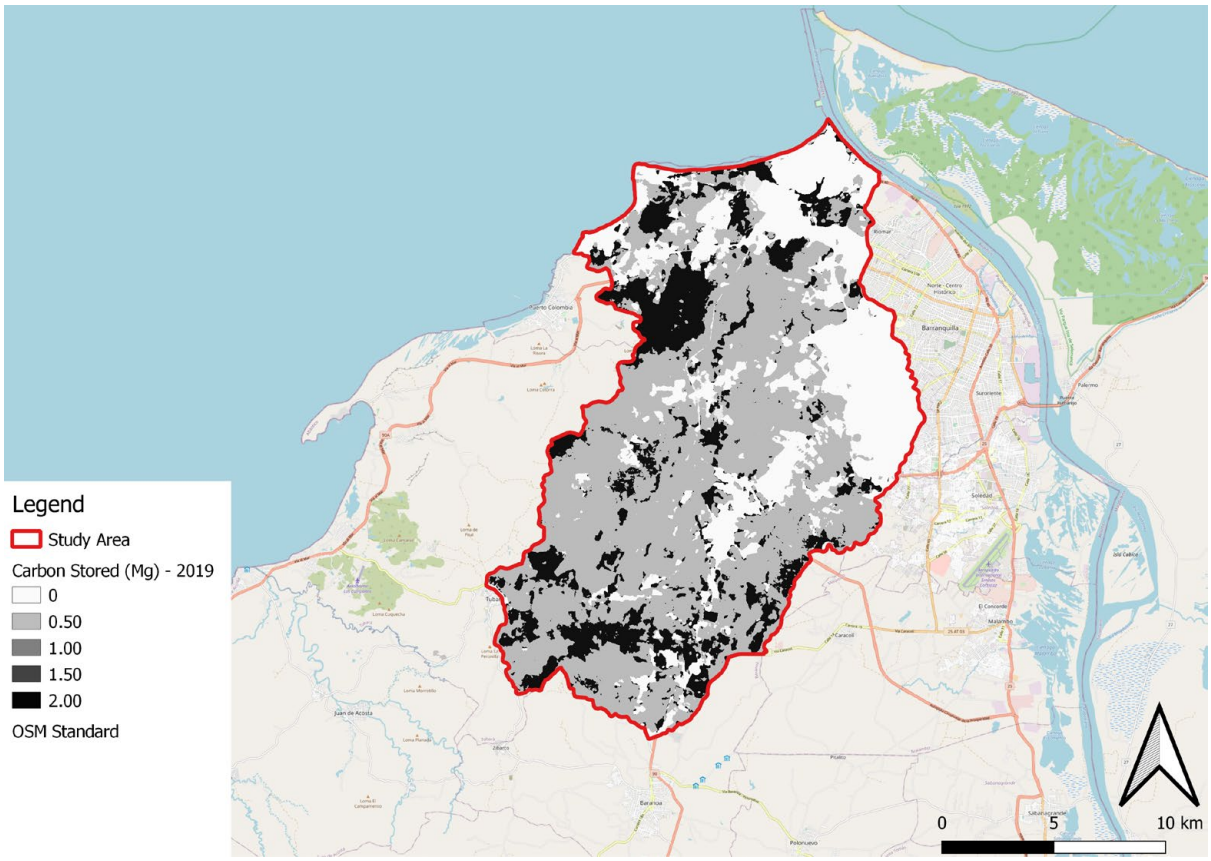

Source: Authors' diagram.

Figure B7. Carbon model outputs (LULC 2021).

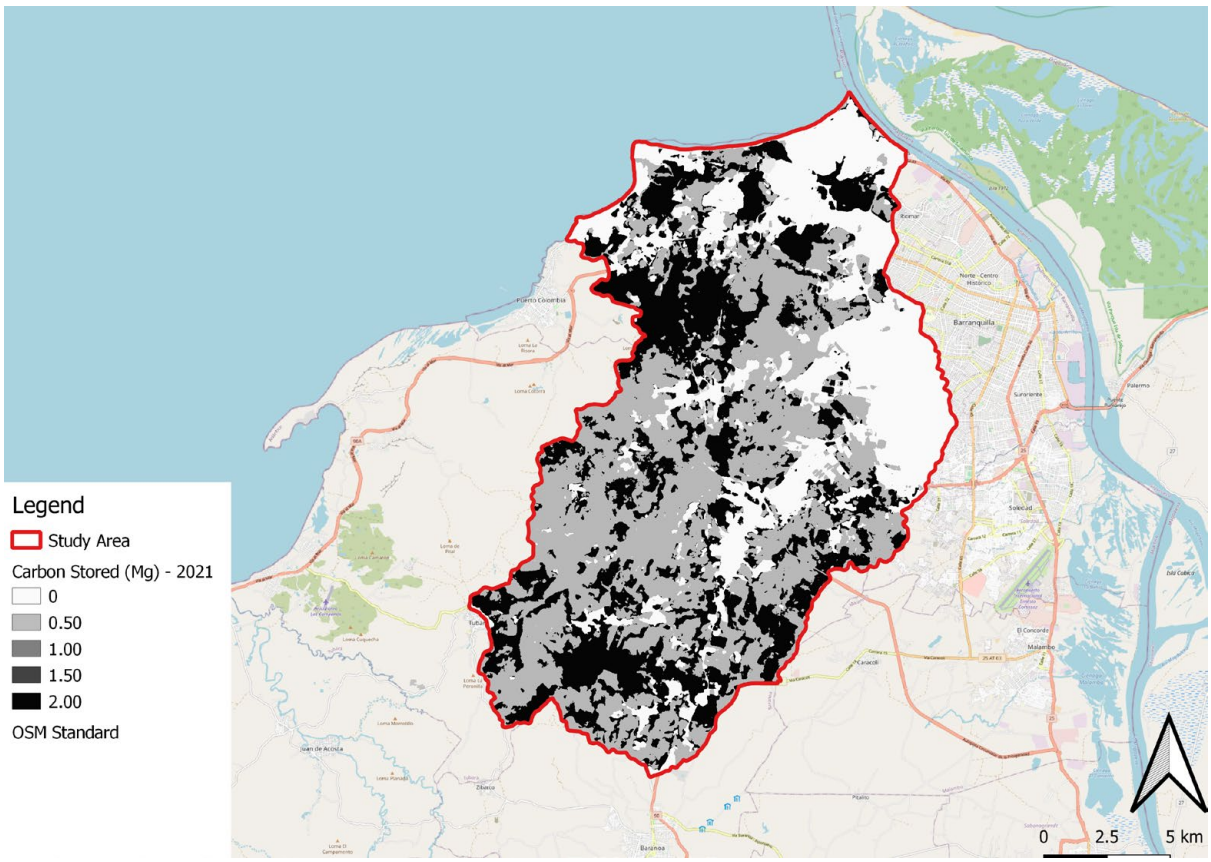

Source: Authors' diagram.

Table B3. Carbon storage statistics

Year	Carbon stored (Mg)	Change from 2017
2017	2,869,487	
2019	1,902,819	-33.69%
2021	2,404,705	-16.20%

As Table B3 shows, from 2017 to 2019 the amount of carbon stored (Mg) has decreased by 33.69%, suggesting that deforestation activities have occurred during this period. On the other hand, from 2017 to 2019 the simulation suggests that carbon storage has increased. This result is in line with Table B1, that indicates that from 2019 to 2021 the total ha of trees has increased.

We also calculated in QGIS the difference in carbon storage from 2017 to 2019 (Figure B8), from 2017 to 2021 (Figure B9), and from 2019 to 2021 (Figure B10), to understand where carbon storage has changed during the years.

Figure B8. Carbon storage change (2017–2019).

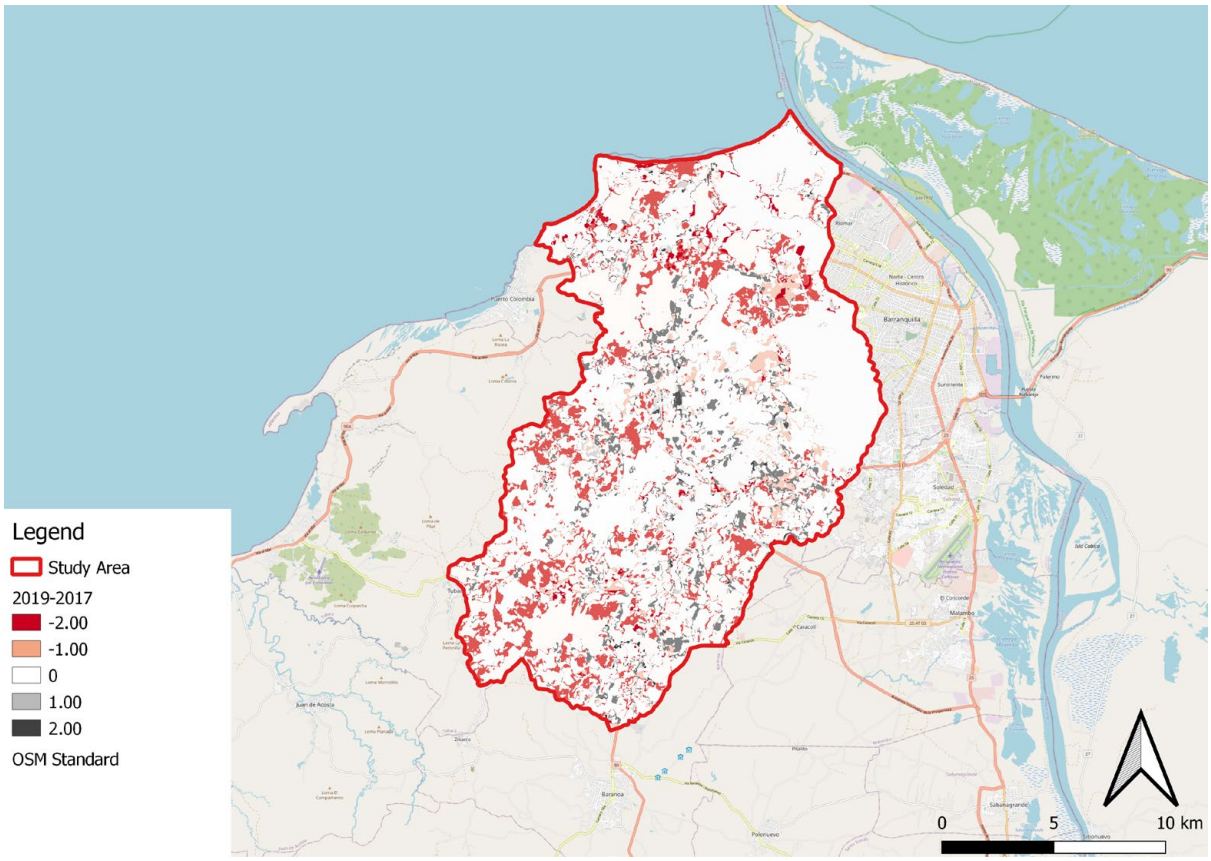

Source: Authors' diagram.

Figure B9. Carbon storage change (2017–2021).

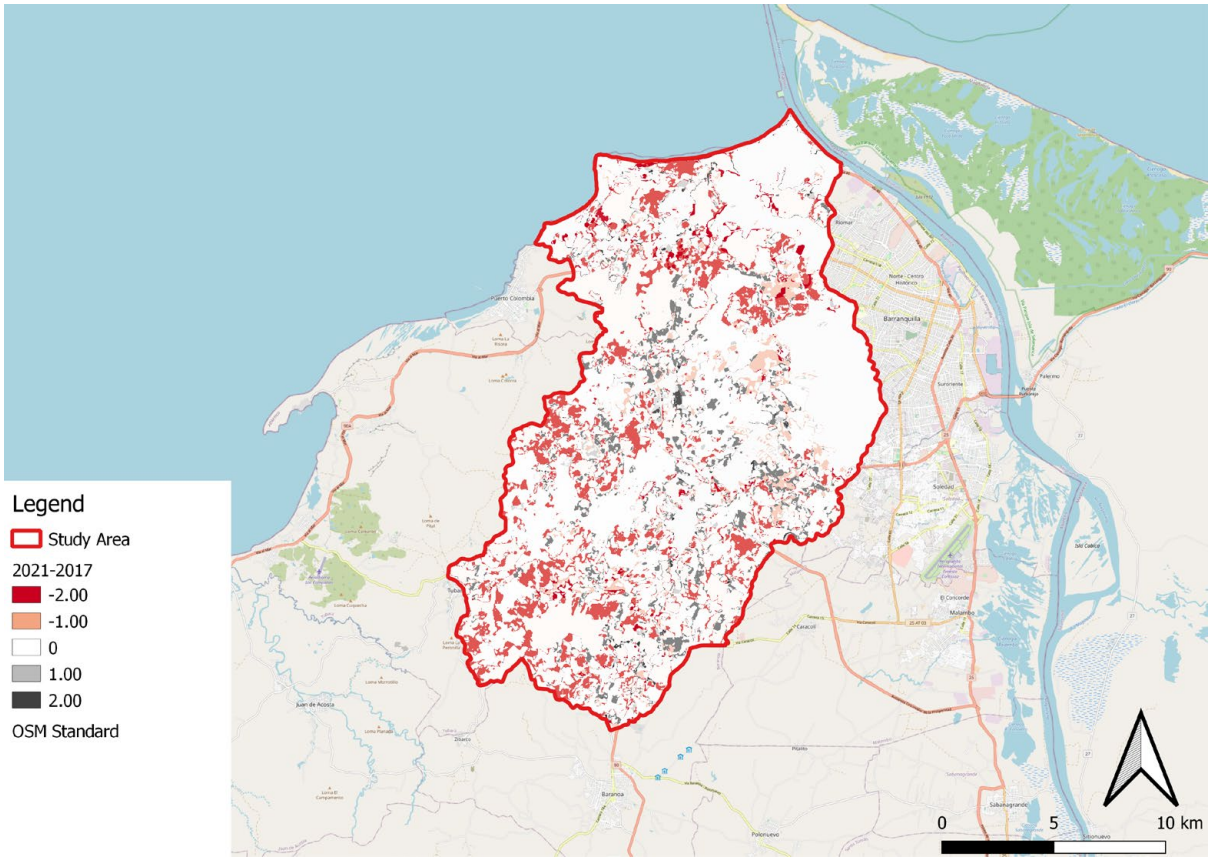

Source: Authors' diagram.

Figure B10. Carbon storage change (2019–2021).

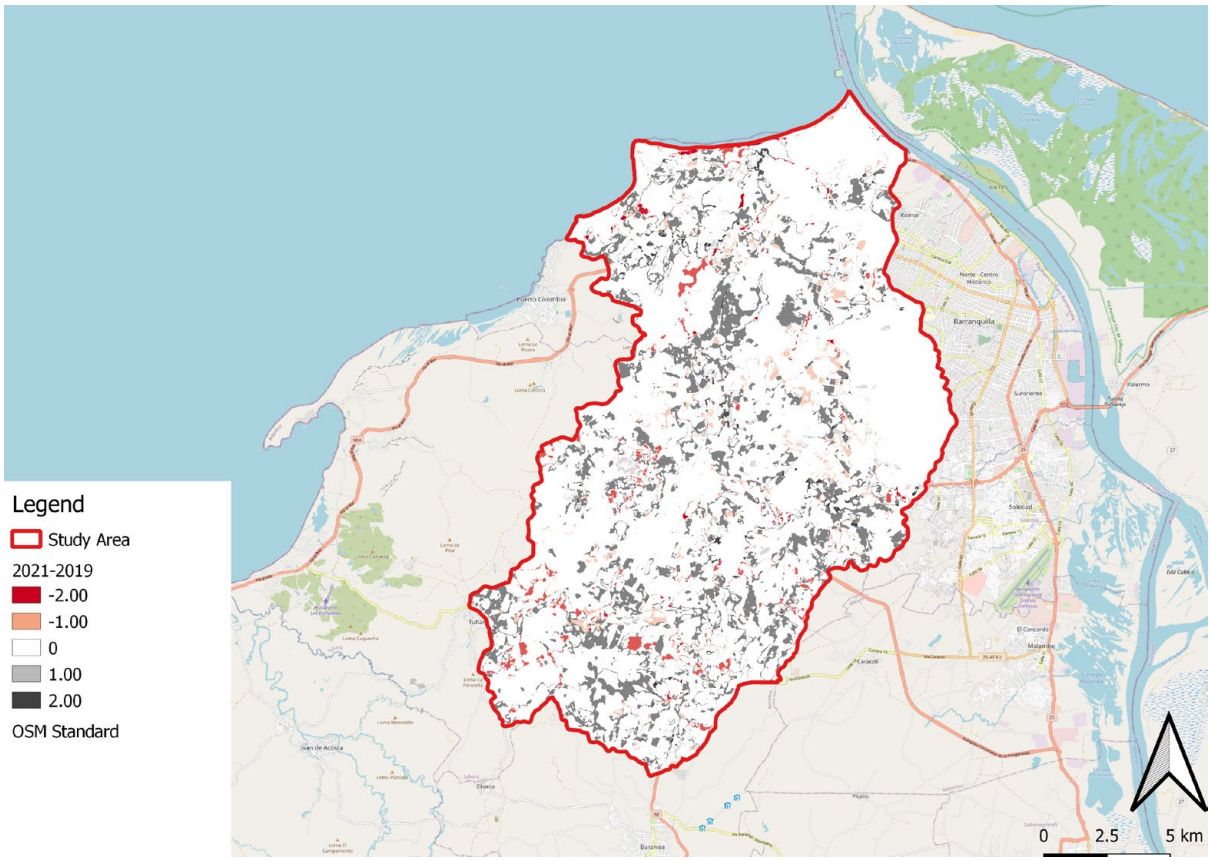

Source: Authors' diagram.

3. Habitat Quality

a. Input Data Preparation and Processing

1. **LULC maps:** See Section 11.c
2. **Threat Data:** Several major threads, such as cropland areas, urban areas, and the road network have been identified as the threat sources to the natural habitat and biodiversity. See Table B4. See Table B10 for data sources.

Table B4. Table of threat (maximum distance, weighted value, and decay function) for InVEST simulation

THREAT	MAX_DIST	WEIGHT	DECAY	CUR_PATH
crop_5	4	0.7	linear	crop_5_c.tif
crop_11	0.5	0.3	linear	crop_11_c.tif
urb_7	7.1	0.7	linear	urb_7_c.tif

3. **Sensitivity of land cover types to each threat:** Table B5 characterizes each LULC type to be habitat or non-habitat and the type's sensitivity to the threats (see Table B11). The table contains the following fields:

   3.1 LULC – codes identify each LULC class

   3.2 Name – abbreviation of each LULC class

   3.3 Habitat – score characterizing each LULC as habitat or non-habitat. The values of 0 and 1 are used for the purpose, in which 0 for non-habitat class and 1 for habitat class of LULC.

Table B5. Table of sensitivity of land cover types to each threat for InVEST simulation

LULC	NAME	HABITAT	crop_5	crop_11	urb_7
1	lc_1	0.3	0.7	0.7	0.8
2	lc_2	1	1	1	1
4	lc_4	1	1	1	1
5	lc_5	0.4	0.03	0.03	0.69
7	lc_7	0	0	0	0
8	lc_8	0	0	0	0
9	lc_9	0	0	0	0
10	lc_10	0.4	0.03	0.03	0.69
11	lc_11	0.4	0.03	0.03	0.69

4. **Half-saturation constraint –** the default value of 0.5 was used

b. Results

Figure B11, Figure B12, and Figure B13 show the relative level of habitat quality in Barranquilla in 2017, 2019, and 2021 respectively. Higher numbers indicate better habitat quality vis-a-vis the distribution of habitat quality across the rest of the landscape. Areas on the landscape that are not habitat get a quality score of 0. The habitat score values range from 0 to 1, where 1 indicates the highest habitat suitability.

Figure B11. Scores of habitat quality – 2017.

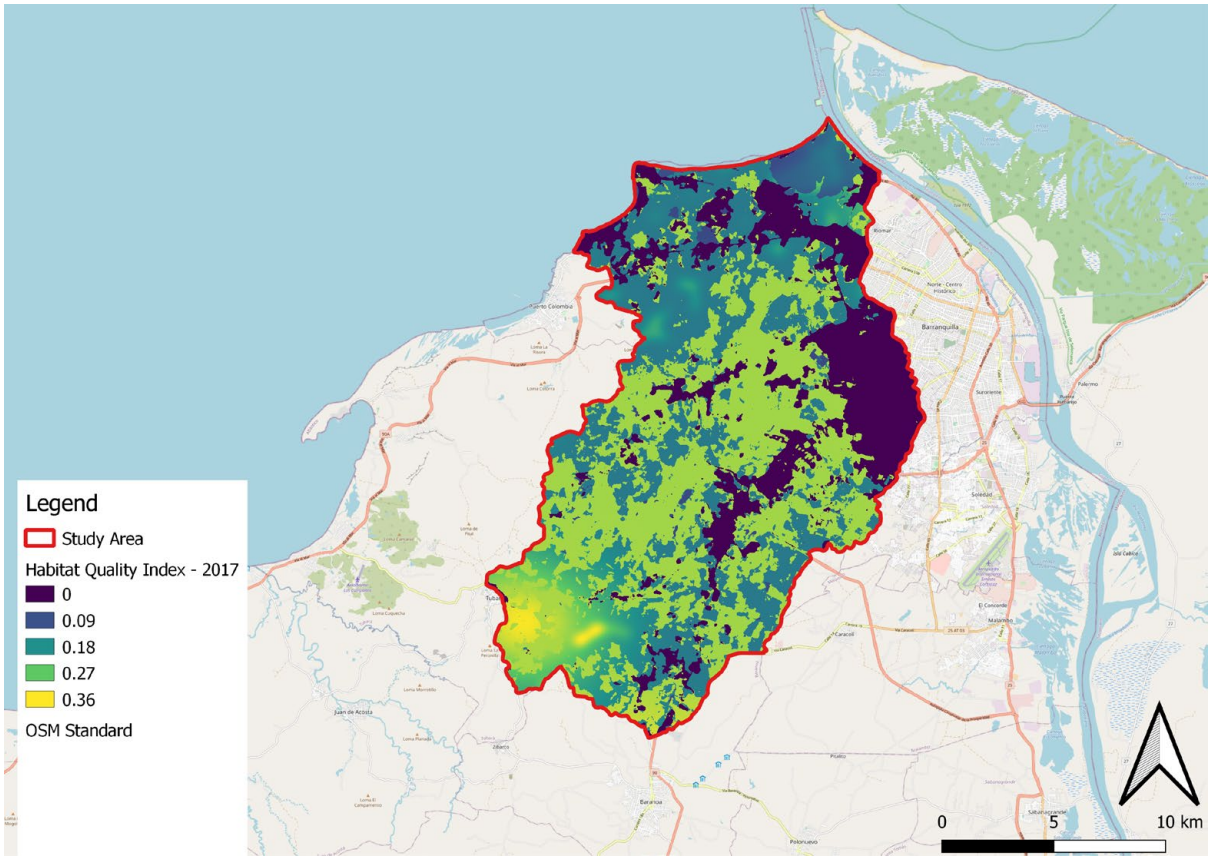

Source: Authors' diagram.

Figure B12. Scores of habitat quality – 2019.

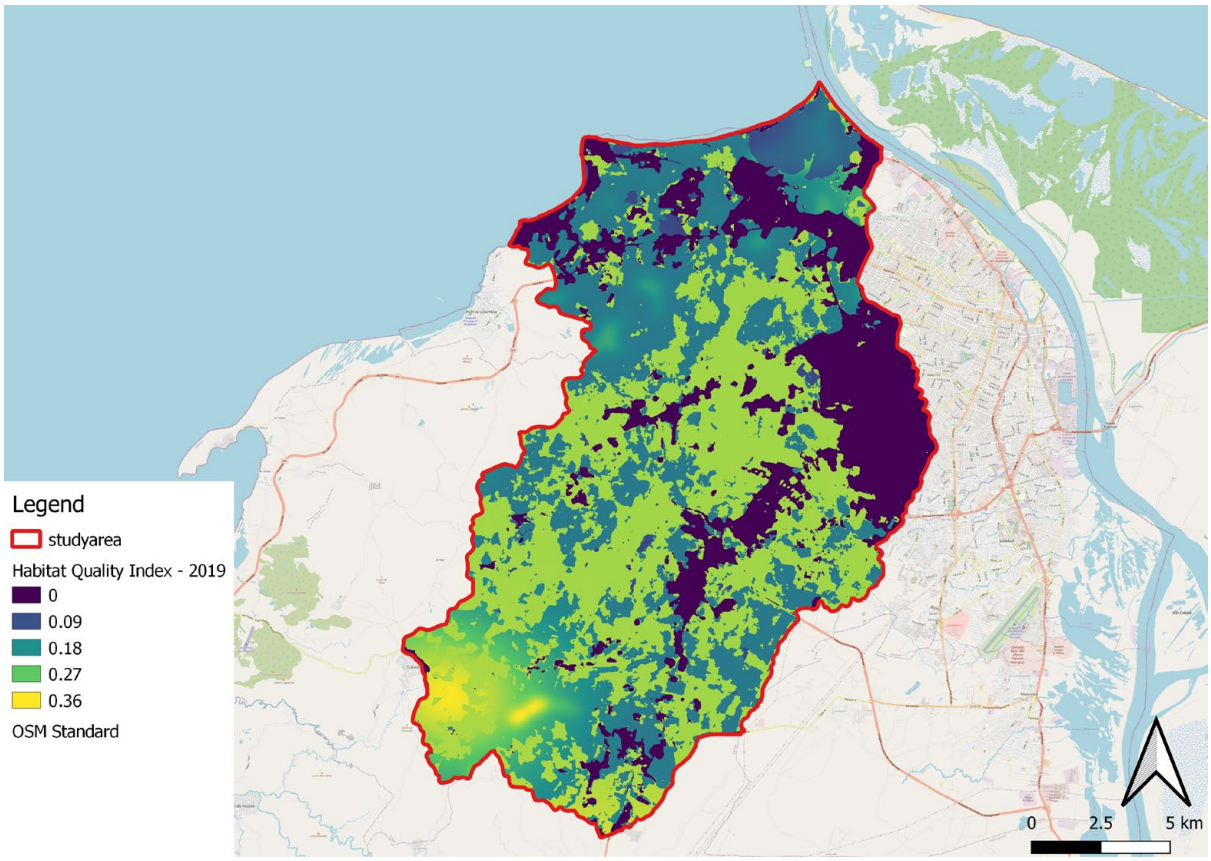

Source: Authors' diagram.

Figure B13. Scores of habitat quality – 2021.

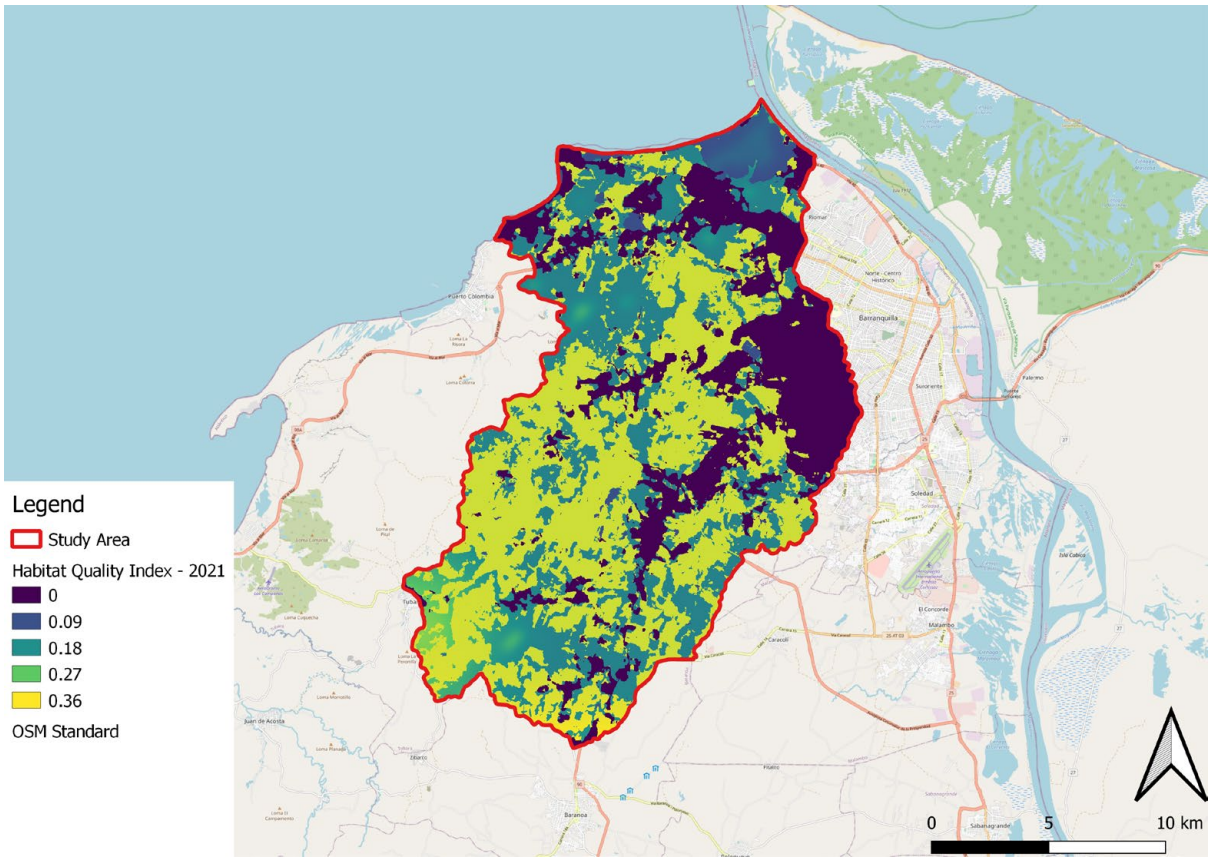

Source: Authors' diagram.

Table B6. Mean of HQ per year

Year	Mean of HQ	Change from 2017
2017	0.205	
2019	0.183	-10.56%
2021	0.189	-7.85%

As Table B6 shows, from 2017 to 2019 the mean in habitat quality decreased by more than 10%, and by more than 7% from 2017 to 2021 due to a decrease in forest land. However, habitat quality improved from 2019 to 2021. This result is in line with Table B1, indicating that from 2019 to 2021 the total ha of trees increased.

4. Nutrient Export

a. Input Data Preparation and Processing

1. **DEM Raster:** See input section of Annual Sediment Delivery Ratio.
2. **LULC maps:** See Section 11.c
3. **Nutrient Runoff Proxy Raster (Precipitation):** A GIS raster dataset with a non-zero value for average annual precipitation for each cell. Its value is in millimetres. The average precipitation (in mm) from 1970 to 2000, downloaded from WorldClim version 2 (www.worldclim.com), was used for this study. The dataset was released on June 1, 2016. The original spatial resolution of the data is 30 seconds x 30 seconds (which is approximately 1 km^2).
4. **Watershed Polygons:** This is the polygon shapefile representing the watersheds
5. **Biophysical Table:** A table of LULC classes containing data on water quality coefficients used in this tool (Table B7). NOTE: these data are attributes of each LULC class rather than attributes of individual cells in the raster map. These data were derived from Kulsoontornrat & Ongsomwang (2021). The table has the following field:

   5.1 Lucode: Unique identifier for each LULC class.

   5.2 load_n / load_p – The nutrient loading for each land use. If nitrogen is being evaluated, supply values in load_n, for phosphorus, supply values in load_p. The potential for terrestrial loading of water quality-impairing constituents is based on nutrient export coefficients. The nutrient loading values are given as integer values and have units of kg. ha-1 yr -1.

   5.3 eff_n / eff_p – The vegetation filtering value per pixel size for each LULC class, as an integer percent between zero and 1. If nitrogen is being evaluated, supply values in eff_n, for phosphorus, supply values in eff_p. This field identifies the capacity of vegetation to retain nutrients, as a percentage of the amount of nutrient flowing into a cell from upslope. For example if the user has data describing that a wetland of 5,000 m^2 retains 82% of nitrogen, then the retention efficiency that they should input into this field for eff_n is equal to (82/5,000 * (cell size)^2). In the simplest case, when data for each LULC type are not available, high values (60 to 80) may be assigned to all natural vegetation types (such as forests, natural pastures, wetlands, or prairie), indicating that 60%–80% of nutrients are retained. An intermediary value also may be assigned to features such as contour buffers. All LULC classes that have no filtering capacity, such as pavement, can be assigned a value of zero.

5.4 crit_len_n (andlor crit_len_p) (at least one is required): The distance after which it is assumed that a patch of a particular LULC type retains nutrients at its maximum capacity, given in metres. If nutrients travel a distance smaller than the retention length, the retention efficiency will be less than the maximum value *eff_x*, following an exponential decay.

This value represents the typical distance necessary to reach the maximum retention efficiency. It was introduced in the model to remove any sensitivity to the resolution of the LULC raster. In the absence of local data for land uses that are not forest or grass, it is possible to simply set the retention length constant, equal to the pixel size: this will result in the maximum retention efficiency being reached within a distance of only one pixel.

5.5 proportion_subsurface_n or p (optional): The proportion of dissolved nutrients over the total amount of nutrients, expressed as a floating point value (ratio) between 0 and 1. By default, this value should be set to 0, indicating that all nutrients are delivered via surface flow.

Table B7. Biophysical table – annual nutrient delivery ratio

lucode	load_n	eff_n	load_p	eff_p	crit_ len_n	crit_ len_p	proportion_ subsurface_n
1	0	0.02	0	0.02	10	10	0
2	2.89	0.51	0.077	0.51	10	10	0
4	2.89	0.51	0.077	0.51	10	10	0
5	11.925	0.13	1.14	0.13	10	10	0
7	6.316	0.03	1.818	0.03	10	10	0
8	0.035	0.05	0.001	0.05	10	10	0
9	0.035	0.05	0.001	0.05	10	10	0
10	11.925	0.13	1.14	0.13	10	10	0
11	13.361	0.13	4.195	0.13	10	10	0

6. **Threshold flow accumulation value:** Integer value defining the number of upstream pixels that must flow into a pixel before it is considered part of a stream. This is used to generate a stream layer from the DEM. This threshold expresses where hydrologic routing is discontinued, that is, where retention stops and the remaining pollutant will be exported to the stream. The value of 10 was used in this simulation.
7. **Subsurface maximum retention efficiency (nitrogen or phosphorus):** the maximum nutrient retention efficiency that can be reached through subsurface flow,

a value between 0 and 1. This field characterizes the retention due to biochemical degradation in soils. The default value of 0.8 was used for this study.

8. **Subsurface_crit_len (nitrogen or phosphorus) (in metres):** The distance (travelled subsurface and downslope) after which is assumed that soil retains nutrient at its maximum capacity. If dissolved nutrients travel a distance smaller than subsubsurface_crit_len, the retention efficiency is lower than the maximum value defined above. A value of 10 was used in this simulation.
9. **Borselli k parameter:** calibration parameter that determines the shape of the relationship between hydrologic connectivity (the degree of connection from patches of land to the stream) and the sediment delivery ratio (percentage of soil loss that actually reaches the stream). The default value is 2.

b. Results

Table B8. Nitrogen Export Statistics

Year	Nitrogen export (kg)	Change from 2017
2017	59,591	
2019	83,902	40.79%
2021	70,009	17.48%

Table B9. Phosphorus export statistics

Year	Phosphorus export (kg)	Change from 2017
2017	16,464	
2019	25,051	52.16%
2021	20,151	22.40%

Table B8 and Table B9 show that the total export of both nitrogen and phosphorus (kg) has increased from 2017 to 2019 (+40.79% and +52.16%, respectively). The decrease in forest cover may be linked to an increase in nutrient exports, and further research may be required to assess the consequences of such findings. On the other hand, from 2019 to 2021 the simulation suggests that the nitrogen and phosphorus exports have decreased. These

results are in line with Table B1, which indicates that from 2019 to 2021 the total ha of trees has increased.

5. Habitat Quality Threat Tables

Table B10. Habitat quality model – references "threat table"

Threat	Max_ Distance	Max_ Distance adopted sources	Weighted value	Weight value adopted sources	Decay function	Decay func. Adopted sources
Crops	4 km	(Terrado et al., 2016)	0.7	(Bhagabati, et al., 2012)	Linear	(Bhagabati, et al., 2012)
Rangeland	0.5 km	(Ciobotaru, et al., 2019)	0.3	(Ciobotaru et al., 2019)	Linear	(Ciobotaru et al., 2019)
Urban areas	7.1 km	(Terrado et al., 2016)	0.7	(Bhagabati, et al., 2012)	Linear	(Bhagabati, et al., 2012)

Table B11. Habitat quality model – references "threat sensitivity table"

Type of habitat	Habitat score	Habitat adopted sources	Sensitivity to agricultural source	Sensitivity to agricultural sources	Sensitivity to urban areas sources	Sensitivity to urban sources
Agriculture and rangeland	0.4	(Terrado et al., 2016)	0.03	(Terrado et al., 2016)	0.69	(Terrado et al., 2016)
Forest	1	(Bhagabati et al., 2012)	1	(Bhagabati et al., 2012)	1	(Bhagabati et al., 2012)
Water	0.3	(Sulistyawan et al., 2017)	0.7	(Sulistyawan et al., 2017)	0.8	(Sulistyawan et al., 2017)
Others, including urban areas	0	(Sulistyawan et al., 2017)	0	(Sulistyawan et al., 2017)	0	(Sulistyawan et al., 2017)

Appendix C. System Dynamics Model Documentation

1. Land Cover

The swamp is classified into three land cover classes: 1) mangroves, 2) mangrove seedlings, and 3) other swamp. At the start of the simulation (1980), we assume there are 46 hectares of mangrove seedlings, 230 hectares of mature mangroves (approximately reproducing observations from (Villate Daza et al., 2020)), and 850 hectares of other swamp. Mangroves naturally colonize 0.27% of the swamp per year. These parameters and initial conditions were tuned to approximately reproduce observations from (Villate Daza et al., 2020). If salinity is less than 5 g/kg or greater than 50 g/kg, the colonization rate decreases (Figure C1).

When restoration is undertaken, mangrove seedlings are planted on 2.89 hectares of swamp in 2019 (Barranquilla Verde, 2021). In 2021, 1.99 times as many seedlings were planted as in 2021 (Barranquilla Verde, 2021). Thus, we estimate 5.75 hectares of seedlings are planted in 2021.

For the planted seedlings, we use a survival rate of 0.81 per year. That is, 19% of the planted seedlings die each year until they mature. Seedlings that survive reach maturity after 20 years (Bernal et al., 2017). The seedling survival rate is estimated to match the observation that 501 days (1.4 years) after the 2019 planting, 74.4% of seedlings had survived (Barranquilla Verde, 2021). The survival rate decreases if salinity is less than 5 g/kg or greater than 50 g/kg (Figure C1).

Under ideal conditions, we assume that mature mangroves live for 100 years. The lifespan decreases if salinity is less than 5 g/kg or greater than 50 g/kg (Figure C1).

Figure C1. Effect of salinity on mangrove survival. The maximum colonization rate, seedling survival rate, and mangrove life span are multiplied the effect of salinity given the current salinity. This graph is estimated from the observation that optimal salinity for mangroves is 5-50 g/kg (Villate Daza et al., 2020).

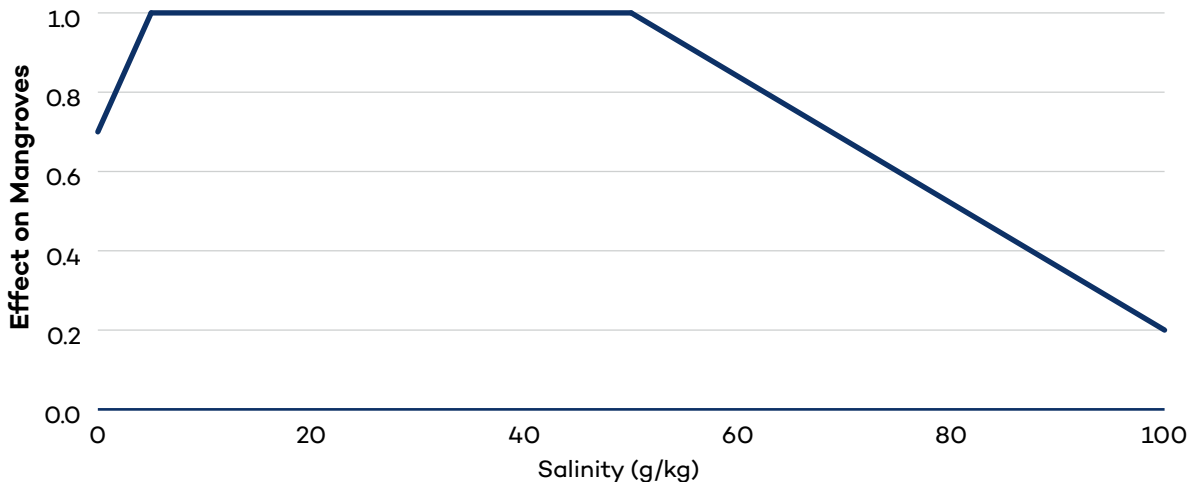

Source: Authors' diagram.

The swamp erodes at a rate that is proportional to the total water level (sea level rise plus wave height). The loss of swamp per mm of water height is calibrated to roughly match observations of swamp extent reported by (Barranquilla Verde, 2021). This calibration produces a rate of 0.0051% per mm of sea level rise per year. Table C1 compares these observations to the simulated extent from 1985 through 2017.

Table C1. Observed and simulated swamp extent

Year	Observed extent (ha)	Simulated extent (ha)
1985	1,065	1,061
1989	998	1,011
1997	891	916
2003	830	847
2011	722	761
2017	694	693

Mangroves disappear at a rate that depends on the difference between sea level rise and accretion due to organic matter and mineral sediments. Following Morris et al. (2016), we assume that organic matter accretion is equal to the belowground productivity of the mangroves (assumed to be 474 g/m^2/year (Giraldo Sánchez, 2005)) multiplied by the share of lignin (assumed to be 10% (Morris et al., 2016)) and a constant organic accretion rate (assumed to 0.085 g/cm^3) (Morris et al., 2016).

Mineral vertical accretion is equal to the mass of sediment retained multiplied by a constant mineral accretion rate (assumed to be 1.99 g/cm^3 (Morris et al., 2016)) divided by the area of mangroves. Sediment retention depends on the sediment load from the Magdalena River. The average discharge from the Magdalena River is 7,100 m^3/s, and the average sediment load is 144.2 million tons per year (Restrepo et al., 2006). To estimate the sediment load in each time step, we multiply the simulated river discharge by 144.2 million tons per year and divide by 7,100 m^3/s. We estimate the share of sediment retained based on the area of mangroves and a constant parameter that is calibrated so that approximately 60% of the total accretion is due to organic matter (Morris et al., 2016).

The change in the elevation of the mangroves is equal to the organic accretion plus the mineral accretion minus sea level rise. If the mangrove elevation is below sea level, mangroves are lost at a rate that is proportional to the depth of sea water. For mangrove loss, we use the same rate as that for the rest of the swamp and assume 0.0051% of mangroves are lost per mm of water per year.

As population grows, settlement area encroaches on the swamp. We use data from the Government of Colombia to estimate population growth rate and assume that there are 17,206 people living in the swamp in 2022 (H. Donado, personal communication, November 17, 2021). We assume that each person requires 0.00406 hectares of land. This estimate comes from an observation that from 1957 through 1993, the population of Barranquilla grew from 399,000 to 1,302,000 (United Nations, Department of Economic and Social Affairs, Population Division, 2018), and the city expanded by 3,672 hectares (Aldana-Domínguez et al., 2018). We divide 3,672 hectares by 903,000 (1,302,000 - 399,000) people to get 0.00406 hectares per person.

We assume that the share of formal vs. informal development depends on water quality, specifically nitrogen and phosphorus pollution. We calibrate the impact of water quality on development to match the observation that before 1993, approximately 63% of development was in informal settlements (Aldana-Domínguez et al., 2018). Informal settlements can also be converted to formal settlements at a rate that increases as water quality improves. We assume that the maximum rate of conversion is 1% per year.

Furthermore, when restoration is undertaken, 10% of informal settlements are relocated each year to allow the swamp to reclaim that area.

2. Flood and Erosion Damage

Total water level is equal to sea level plus the wave significant height. Sea level rise scenarios are taken from Sweet et al. (2022). We use linear regression to determine a relationship between observed historical wind speed provided by Hersbach et al. (2019) and sea surface wave significant height provided by E.U. Copernicus Marine Service Information (2019). This gives us the following formula to predict future wave significant height: 0.135 × wind speed + 0.413, where wind speed is taken from Copernicus Climate Change Service (2018).

We assume that each metre of mangroves reduces the water level by 0.3%. This assumption comes from the observation that wave height is reduced by 13%–66% per 100 m of mangroves (Spalding et al., 2014). We estimate the width of mangroves by dividing the area by the length of the fringe. We subtract the effect of mangroves from the total water level to determine the effective water level.

Settlement area erodes at a rate that depends on the effective water level. Garza & Lizieri (2015) report an average value of COP 496,966 per square metre of built environment in Barranquilla. Converting to USD per hectare, we therefore assume that each hectare of formal settlements has a monetary value of USD 1.32 million. For informal settlements, we consider the value of the land, rather than the built environment. Garza & Lizieri (2015) report land values of COP 38,000 through COP 400,000 per square metre throughout the city. We assume that the informal settlements will have one of the lowest land values and so, converting to USD per hectare, we assume a value of USD 120,000 per hectare of informal settlements. Erosion damage is calculated as the product of area lost and value per hectare.

To calculate flood damage, we define a threshold for the effective water level, assumed to be 0.5 m. We assume that at the flood threshold damages are equal to 10% of formal settlement value added to 20% of informal settlement value. The percentage destroyed in each flood event increases in proportion to the height of the water above the threshold.

3. Carbon Storage

We assume that, at the start of the simulation, mangroves store 150 tons of CO_2 per hectare (Kauffman et al., 2020). We simulate the change in carbon storage based on the change in land cover. Under ideal salinity conditions, mangrove seedlings sequester 16.1 tons of CO_2 per hectare per year and mature mangroves sequester 7.4 tons of CO_2 per hectare per year (Bernal et al., 2017). To account for high or low salinity, we multiply these sequestration rates by the effect of salinity shown in Figure C1.

As mangroves are converted to settlements or die of natural causes, they release carbon into the atmosphere.

4. Fisheries

We assume that fish landings depend on the length of the mangrove fringe, which is equal to the square root of the area of mangroves (in km^2) multiplied by 6.13 (Aburto-Oropeza et al., 2008). In Mexico, a study found that each kilometre of mangrove fringe produced USD 25,149 worth of fish annually and that 11,600 tons are worth USD 19 million (Aburto-Oropeza et al., 2008). From this, we calculate USD 25,149 per km per year × 11,600 tons per USD 19 million = 15.35 tons per km per year. Fishing income is equal to fish landings multiplied by income per ton. We estimate a value of USD 2,298 per ton based on country-specific data for Colombia from Organisation for Economic Co-operation and Development (2021).

5. Tourism

If ecotourism infrastructure is built, the area could see an increase in tourism of 6,928 visitors per day, equivalent to 2.53 million visitors per year (M. Castillo Ramírez & G. Serrano Aragundi, personal communication, October 10, 2022). We assume that each visitor will spend, on average, COP 42,000 (USD 11.16) on food, beverages, and transportation and that there will be additional revenue of COP 1,002 million (USD 266,000) from other sources (Monroy & Salazar, 2021).

To test the outcome if there are fewer visitors, we use a lower estimate of 900,000 visitors per year. This is a central value of the total national, international, and local visitors estimated by (Monroy & Salazar, 2021) and excludes touristic train rides. We again assume spending per visitor of COP 42,000 (USD 11.16) and include additional revenue of COP 4,972.5 million (USD 1.32 million) from the tourist train and COP 1,002 million (USD 266,000) from other sources (Monroy & Salazar, 2021).

For both the high and low tourism scenarios, we assume that the increase in visitors starts in 2024 (i.e., it takes 5 years for the infrastructure to be built).

If no ecotourism infrastructure is built, we assume that the costs of NBI are reduced by 50% and that there is no increase in tourism revenue.

6. Water Quality

We assume that each hectare of informal settlements in the swamp produces 500 kg of nitrogen and 55 kg of phosphorus annually. Formal settlements produce 50 kg of nitrogen and 6 kg of phosphorus. There is also a constant input of 30,000 kg of nitrogen and 3,300 kg of phosphorus from exogenous sources. These parameters are estimated to be approximately aligned with two water quality observational studies of the Mallorquín Swamp. The first found that total nitrogen concentration is up to 20 milligrams per litre (mg/L) in the dry season and below 3 mg/L during the rainy season and that total phosphorus concentration is between 1.4 mg/L and 3.43 mg/L (Corporación Autónoma Regional del Atlántico, 2018). The second found that total phosphorus was between 0.23 mg/L and 10.83 mg/L, and total nitrogen was less than 5 mg/L, depending on sample site and day (Establecimiento Público Ambiental, 2020).

Based on a study conducted on the southeast coast of China, we assume that each hectare of mangroves removes 905 kg of nitrogen and 22 kg of phosphorus per year (Wang et al., 2010).

Concentration of nutrients is equal to the accumulated mass divided by the volume of water in the swamp.

Water volume increases with fresh water from the Leon and Magdalena Rivers, precipitation, and tidal inflow. Evaporation and outflow to the sea (due to tides and flushing) decrease water volume.

For the Magdalena River, the average annual minimum discharge is 4,068 m^3/s (Restrepo et al., 2006). To estimate monthly discharge, we add this number to an estimated impact of precipitation on discharge. This impact is equal to monthly precipitation divided by the monthly average precipitation (105 mm) multiplied by 2,700, which is a parameter tuned so that the historical maximum discharge matches the observed maximum of close to 15,000 m^3/s (Restrepo et al., 2006). Finally, we assume that due to port construction, only 0.0056% of the river discharge enters the swamp. This parameter was estimated so that water inflow matches the observation that structures built in 1992 allow an average of 1 m^3/s through but that due to lack of maintenance, the actual supply may only be 0.35-0.5 m^3/s (Páez Correa, 2015). When restoration is undertaken, we assume that the percentage of water flow that reaches the swamp increases to 1.0%.

For the Leon River, we follow the same process using an average minimum monthly discharge of 20 m^3/s and calibrating the equations so that monthly maximum flow is approximately 100 m^3/s (Alzate et al., 2015). We assume that 50% of the flow from the Leon River enters the swamp. These parameter values result in an average water depth of approximately 1 m, which is the depth reported by Barranquilla Verde (2021).

The depth of precipitation and evaporation are converted to volumes by using the area of the swamp.

The (non-tidal) outflow is equal to the volume in the swamp divided by the flushing time, which we assume is 5 days at the start of the simulation and changes proportional to the area of the swamp.

We calculate the tidal prism (i.e., the volume of water that enters and exits the swamp in each tidal cycle) as the total swamp area multiplied by the difference between high and low tide (i.e., the "tidal range"), for which we use a value of 45 centimetres (Pickering et al., 2017).[1] We further assume a tidal period of 0.5 days. Note that because the model takes monthly time steps we do not observe tidal variations in the model output, but including this dynamic is critical for estimating the salinity of the swamp.

We assume that the salinity of the sea is 34 g/kg (Beier et al., 2017). Thus, in each tidal cycle the mass of salt that enters the estuary is equal to the volume of the tidal inflow multiplied by 34 g/kg times the density of water (assumed to be 1 kg/m^3 increased by a percentage equal to the salinity measured in kg per kg of water). The salinity in the swamp is calculated as the mass of salt divided by the volume of water. The outflow of salt is equal to the salinity of the swamp multiplied by the total water outflow (flushing and tidal) times the density of water.

7. Grey Infrastructure

We simulate three types of grey infrastructure that performs services similar to mangroves:

- An offshore breakwater to mitigate flooding and erosion
- A wastewater treatment plant to improve water quality
- Renewable energy to mitigate greenhouse gas emissions

We assume that the breakwater is constructed along 5 km of coastline at a depth of approximately 1.2 m. To achieve similar erosion/flood mitigation benefits as planting mangroves and relocating informal settlements, the breakwater must reduce wave height by 0.17 m under RCP 4.5 and 0.21 m under RCP 8.5.

For the wastewater treatment plant to have similar water quality benefits as restoring mangroves and relocating informal settlements, it must have a capacity of 485,000 m^3 per day under RCP 4.5 and 495,000 m^3 per day under RCP 8.5. Wastewater flow is equal to the lesser of the capacity and the freshwater inflow per day. We further assume that the plant is 100% effective at removing nitrogen and phosphorus from the wastewater that enters it. We assume that the percentage of the total accumulated nitrogen and phosphorus production removed by the wastewater treatment plant is equal to the wastewater flow divided by the freshwater inflow to the swamp.

To calculate emissions reductions from installed solar panels, we assume a current electricity carbon intensity of 0.182 kg CO_2/kWh, which is equal to the national average for Colombia (Climate Transparency, 2020). Thus, we estimate that 182 g CO_2 per kWh × 8,760 hours per year / 1,000,000 g per ton = 1.59 tons CO_2 avoided per year per kW of solar power generation. We then estimate that 633.5 kW of solar power generation must be installed to reduce emissions to the same extent as mangrove restoration over 20 years under the RCP 4.5 climate scenario. For RCP 8.5, 774.6 kW of solar power generation must be installed.

[1] Pickering et al. (2017) found that with 2 metres of sea level rise, the tidal range in Barranquilla could increase up to 8 centimetres if coastal recession occurs, but this increase is not proportional to sea level rise. This means that this result cannot be extrapolated to other amounts of sea level rise. Furthermore, with no coastal recession, the same study found that the tidal range in Barranquilla will not change with 2 metres of sea level rise. We, therefore, assume that the tidal range remains constant over the course of the simulation.

We also include a scenario in which we assume that tourism infrastructure is built with the breakwater, wastewater treatment plant, and solar panels. In this case, we assume that the cost to invest in tourism is 50% of the cost of the restoration project. We also assume that this would result in the same tourism benefit as the NBI scenario (considering both the high and low tourism estimates).

For all grey infrastructure, we assume that construction takes 5 years.

8. Employment

Jobs are created from building and maintaining the nature-based and grey infrastructure. Planting 2.89 ha of mangroves in 2019 employed 107 people over 15 days (Barranquilla Verde, 2021). Assuming 260 person days per full time equivalent (FTE) job, we get that planting mangroves creates 107 people × 15 days ÷ 260 person days per FTE ÷ 2.89 ha = 2.14 FTE per ha. We assume that seedling maintenance will require 20% of this labour, so in each year after mangroves are planted, the area of planted seedlings creates 0.43 FTE per ha.

For the wastewater treatment plant, we assume that 0.0001 jobs are created for each dollar invested (Schwartz et al., 2009).

To estimate jobs from solar panels, we start with the assumption that the labour price for installation is EUR 43 (USD 49) per kW. We then use an average monthly construction wage in Colombia of USD 291.1 or USD 3,439.2 per year (International Labour Organization, 2022). From this, we estimate that each kW installed creates USD 49 ÷ USD 3,439.2 per FTE = 0.014 FTE per kW.

We assume that constructing the breakwater creates 7 FTE jobs per km and that maintenance creates 3 FTE per km.

For tourism infrastructure (both conventional and ecotourism), we assume that 10% of the tourism construction and maintenance costs go toward wages.

References

Aburto-Oropeza, O., Ezcurra, E., Danemann, G., Valdez, V., Murray, J., & Sala, E. (2008). Mangroves in the Gulf of California increase fishery yields. *Proceedings of the National Academy of Sciences, 105*(30), 10456–10459. https://doi.org/10.1073/pnas.0804601105

Aldana-Domínguez, J., Montes, C., & González, J. (2018). Understanding the Past to Envision a Sustainable Future: A Social–Ecological History of the Barranquilla Metropolitan Area (Colombia). *Sustainability, 10*(7), 2247. https://doi.org/10.3390/su10072247

Alzate, L., Agamez, M., Juan, S., & Julio, M. (2015). *Modification of Environmental License for the Project of Construction and Operation of a Solid Bulk Cargoes Port Terminal in the Municipality of Turbo: Characterization of the Influence Area [Review of Modification of Environmental License for the Project of Construction and Operation of a Solid Bulk Cargoes Port Terminal in the Municipality of Turbo: Characterization of the Influence Area*, by C. Rey & J. Bibiana Salazar]. https://www3.dfc.gov/Environment/EIA/puertoantioquia/ESIA/Chapter_5_1.pdf

Barranquilla Verde. (2021). *Contexto General.*

Beier, E., Bernal, G., Ruiz-Ochoa, M., & Barton, E. D. (2017). Freshwater exchanges and surface salinity in the Colombian basin, Caribbean Sea. *PLOS ONE, 12*(8), e0182116. https://doi.org/10.1371/journal.pone.0182116

Bernal, B., Sidman, G., & Pearson, T. (2017). *Assessment of mangrove ecosystems in Colombia and their potential for emissions reductions and restoration* (p. 29). Winrock International. https://winrock.org/wp-content/uploads/2018/02/6.-Coastal-assessment-in-Colombia.pdf

Bhagabati, N., Barano, T., Conte, M., Ennaanay, D., Hadian, O., McKenzie, E., Olwero, N., Rosenthal, A., Suparmoko, Shapiro, A., Tallis, H., & Wolny, S. (2012). *Using ecosystem services information to make recommendations for sustainable land use planning at the province and district level* (p. 173). The Natural Capital Project, WWF-US, and WWF-Indonesia. https://woodsinstitute.stanford.edu/system/files/publications/GreenVision.pdf

Brand, M. W., Seipp, K. Q., Saksa, P., Ulibarri, N., Bomblies, A., Mandle, L., Allaire, M., Wing, O., Puente, J. T. la, Parker, E. A., Nay, J., Sanders, B. F., Rosowsky, D., Lee, J., Johnson, K., Gudino-Elizondo, N., Ajami, N., Wobbrock, N., Adriaens, P., … Gibbons, J. P. (2021). Environmental Impact Bonds: A common framework and looking ahead. *Environmental Research: Infrastructure and Sustainability, 1*(2), 023001. https://doi.org/10.1088/2634-4505/ac0b2c

Calvo, R. N., & Arispe, S. (2021). *Evaluación Ambiental y Social Estratégica*. Inter-American Development Bank. https://www.barranquilla.gov.co/programa-de-biodiverciudad-y-equidad-urbana-en-barranquilla

Ciobotaru, N., Laslo, L., Lupei, T., Deák, G., Matei, M., Bara, N., & Noor, N. M. (2019). Preliminary assessment of the status of Romanian wetlands through the framework of habitat quality analysis. *AIP Conference Proceedings, 2129*, 020070. https://doi.org/10.1063/1.5118078

Climate Transparency. (2020). *The Climate Transparency Report 2020: Comparing G20 climate action and responses to the COVID-19 crisis*. https://www.climate-transparency.org/g20-climate-performance/the-climate-transparency-report-2020#1531904804037-423d5c88-a7a7

Copernicus Climate Change Service. (2018). CMIP5 monthly data on single level. *Coupled Model Intercomparison Project Phase 5*. https://cds.climate.copernicus.eu/cdsapp#!/dataset/projections-cmip5-monthly-single-levels

Corporación Autónoma Regional del Atlántico. (2018). *Caracterización Fisicoquímica, Microbiológica e Hidrobiológica de Tres Lagunas Costeras en el Departamento del Atlántico y Desarrollo de un Índice de Calidad del Agua Para su Gestión*. Laboratorio para la Industria y el Medio Ambiente LIMA S.A.S. https://www.crautonoma.gov.co/documentos/Monitoreos%20de%20calidad%20de%20agua/INFORME%20Caracterizacion%20%20ICA%20%20C%20000294.pdf

Earth Security. (2021). *The Blended Finance Playbook for Nature* [Strategic Report]. https://www.earthsecurity.org/reports/the-blended-finance-playbook-for-nature-based-solutions

Establecimiento Público Ambiental. (2020). *Informe Técnico de Estudio de Caracterización de Agua Superficial* (p. 125). SERAMBIENTE.

E.U. Copernicus Marine Service Information. (2019). *Global Ocean Waves Reanalysis Waverys*. https://resources.marine.copernicus.eu/?option=com_csw&view=details&product_id=GLOBAL_REANALYSIS_WAV_001_032

Garza, N., & Lizieri, C. (2015). *An empirical approach to land monopoly: The case of Barranquilla, Colombia* (Working paper series no. 2015–03). University of Cambridge, Real Estate Research Centre. http://dx.doi.org/10.2139/ssrn.2807024

Giraldo Sánchez, B. E. (2005). *Belowground productivity of mangrove forests in southwest Florida* [Doctoral Dissertation, Louisiana State University and Agricultural and Mechanical College]. https://digitalcommons.lsu.edu/cgi/viewcontent.cgi?article=2651&context=gradschool_dissertations

Green Finance Institute. (2023). *Blue Forest Conservation Forest Resilience Bond*. Greenfinanceinstitute.Co.Uk. https://www.greenfinanceinstitute.co.uk/gfihive/case-studies/blue-forest-conservation-forest-resilience-bond

Hernández-Sancho, F., Molinos-Senante, M., & Sala-Garrido, R. (2010). Economic valuation of environmental benefits from wastewater treatment processes: An empirical approach for Spain. *Science of The Total Environment, 408*(4), 953–957. https://doi.org/10.1016/j.scitotenv.2009.10.028

Hersbach, H., Bell, B., Berrisford, P., Biavati, G., Horanyi, A., & M. (2019). *ERA5 monthly averaged data on single levels from 1979 to present*. Copernicus Climate Change Service Climate Data Store. https://doi.org/10.24381/cds.f17050d7

Intergovernmental Panel on Climate Change. (2006). *2006 IPCC guidelines for national greenhouse gas inventories* (S. Eggleston, L. Buendia, K. Miwa, T. Ngara, & K. Tanabe, Eds.). Institute for Global Environmental Strategies. https://www.ipcc.ch/report/2006-ipcc-guidelines-for-national-greenhouse-gas-inventories/

International Labour Organization. (2022). Average monthly earnings of employees by sex and occupation—Annual. *ILOSTAT*. https://www.ilo.org/shinyapps/bulkexplorer13/?lang=en&segment=indicator&id=EAR_4MTH_SEX_OCU_CUR_NB_A

Jiang, Y., Dinar, A., & Hellegers, P. (2018). Economics of social trade-off: Balancing wastewater treatment cost and ecosystem damage. *Journal of Environmental Management, 211*, 42–52. https://doi.org/10.1016/j.jenvman.2018.01.047

Kauffman, J. B., Adame, M. F., Arifanti, V. B., Schile-Beers, L. M., Bernardino, A. F., Bhomia, R. K., Donato, D. C., Feller, I. C., Ferreira, T. O., Jesus Garcia, M. del C., MacKenzie, R. A., Megonigal, J. P., Murdiyarso, D., Simpson, L., & Hernández Trejo, H. (2020). Total ecosystem carbon stocks of mangroves across broad global environmental and physical gradients. *Ecological Monographs, 90*(2). https://doi.org/10.1002/ecm.1405

Kulsoontornrat, J., & Ongsomwang, S. (2021). Suitable land-use and land-cover allocation scenarios to minimize sediment and nutrient loads into Kwan Phayao, Upper Ing watershed, Thailand. *Applied Sciences, 11*(21), 10430. https://doi.org/10.3390/app112110430

López, A. R., Krumm, A., Schattenhofer, L., Burandt, T., Montoya, F. C., Oberländer, N., & Oei, P.-Y. (2020). Solar PV generation in Colombia—A qualitative and quantitative approach to analyze the potential of solar energy market. *Renewable Energy, 148*, 1266–1279. https://doi.org/10.1016/j.renene.2019.10.066

Monroy, L. E., & Salazar, A. M. (2021). *Recuperación Integral de La Ciénaga de Mallorquín Una estimación de impactos socioeconómicos*. Sectetaría de Planeación. Alcaldía Distrital de Barranquilla. https://www.barranquilla.gov.co/planeacion/documentos-tecnicos-preliminares

Morris, J. T., Barber, D. C., Callaway, J. C., Chambers, R., Hagen, S. C., Hopkinson, C. S., Johnson, B. J., Megonigal, P., Neubauer, S. C., Troxler, T., & Wigand, C. (2016). Contributions of organic and inorganic matter to sediment volume and accretion in tidal wetlands at steady state. *Earth's Future, 4*(4), 110–121. https://doi.org/10.1002/2015EF000334

Narayan, S., Beck, M. W., Reguero, B. G., Losada, I. J., van Wesenbeeck, B., Pontee, N., Sanchirico, J. N., Ingram, J. C., Lange, G.-M., & Burks-Copes, K. A. (2016). The effectiveness, costs and coastal protection benefits of natural and nature-based defences. *PLOS ONE, 11*(5), e0154735. https://doi.org/10.1371/journal.pone.0154735

Natural Capital Project. (2019). *InVEST*. Natural Capital Project. https://naturalcapitalproject.stanford.edu/software/invest

Oppenheimer, M., Glavovic, B. C., Hinkel, J., van de Wal, R., Magnan, A. K., Abd-Elgawad, R., Cai, R., Cifuentes-Jara, M., DeConto, R. M., Ghosh, T., Hay, J., Isla, F., Marzeion, B., Meyssignac, B., & Sebesvari, Z. (2019). Chapter 4: Sea Level Rise and Implications for Low-Lying Islands, Coasts and Communities. In H.-O. Portner, D. C. Roberts, V. Masson-Delmotte, P. Zhai, M. Tignor, E. Poloczanska, K. Mintenbeck, A. Alegria, M. Nicolai, A. Okem, J. Petzold, B. Rama, & N. M. Weyer (Eds.), *IPCC special report on the ocean and cryosphere in a changing climate*. In press. https://www.ipcc.ch/srocc/chapter/chapter-4-sea-level-rise-and-implications-for-low-lying-islands-coasts-and-communities/

Organisation for Economic Co-operation and Development. (2021). *Fisheries and aquaculture in Colombia*. https://www.oecd.org/agriculture/topics/fisheries-and-aquaculture/documents/report_cn_fish_col.pdf

Páez Correa, C. (2015). Análisis de las dimensiones del desarrollo sostenible en la ciénaga de mallorquín. *Módulo Arquitectura, 14*(2), 63–84.

Pickering, M. D., Horsburgh, K. J., Blundell, J. R., Hirschi, J. J.-M., Nicholls, R. J., Verlaan, M., & Wells, N. C. (2017). The impact of future sea-level rise on the global tides. *Continental Shelf Research, 142*, 50–68. https://doi.org/10.1016/j.csr.2017.02.004

Restrepo, J., Zapata, P., Diaz, J., Garzonferreira, J., & Garcia, C. (2006). Fluvial fluxes into the Caribbean Sea and their impact on coastal ecosystems: The Magdalena River, Colombia. *Global and Planetary Change, 50*(1–2), 33–49. https://doi.org/10.1016/j.gloplacha.2005.09.002

Rojas, F., Hobbs, J., Acevedo, P., Zambrano-Barragán, P., Piedrafita, C., Palacio, M., Chamas, P., Guzman, J., Sandoval, J. M., Salazar, C., Avila, J., Orellana, E., Navarrete, M. J., Cruz, P., Maragall, J., Zegarra, F., Bocarejo, D., Rojas, J., Catacoli, A., … Giraldo, A. (n.d.). *Project Profile: Colombia*. https://www.barranquilla.gov.co/programa-de-biodiverciudad-y-equidad-urbana-en-barranquilla

Schwartz, J. Z., Andres, L. A., & Dragoiu, G. (2009). *Crisis in Latin America: Infrastructure investment, employment and the expectations of stimulus* (Policy research working paper No. 5009). The World Bank. https://openknowledge.worldbank.org/bitstream/handle/10986/4201/WPS5009.pdf

Spalding, M., McIvor, A., Tonneijck, F. H., Tol, S., & van Eijk, P. (2014). *Mangroves for coastal defence: Guidelines for coastal managers and policy makers.* Wetlands International and The Nature Conservancy. https://tamug-ir.tdl.org/bitstream/handle/1969.3/29257/mangroves-for-coastal-defence.pdf?sequence=1

Sulistyawan, B. S., Eichelberger, B. A., Verweij, P., Boot, R. G. A., Hardian, O., Adzan, G., & Sukmantoro, W. (2017). Connecting the fragmented habitat of endangered mammals in the landscape of Riau–Jambi–Sumatera Barat (RIMBA), central Sumatra, Indonesia (connecting the fragmented habitat due to road development). *Global Ecology and Conservation, 9*, 116–130. https://doi.org/10.1016/j.gecco.2016.12.003

Sweet, W. V., Hamlington, B. D., Kopp, R. E., Weaver, C. P., Barnard, P. L., Bekaert, D., Brooks, W., Craghan, M., Dusek, G., Frederikse, T., Garner, G., Genz, A. S., Krasting, J. P., Larour, E., Marcy, D., Marra, J. J., Obeysekera, J., Osler, M., Pendleton, M., … Zuzak, C. (2022). *Global and regional sea level rise scenarios for the United States: Updated mean projections and extreme water level probabilities along U.S. coastlines* (Technical report no. 1). National Oceanic and Atmospheric Administration, National Ocean Service. https://aambpublicoceanservice.blob.core.windows.net/oceanserviceprod/hazards/sealevelrise/noaa-nos-techrpt01-global-regional-SLR-scenarios-US.pdf

Terrado, M., Sabater, S., Chaplin-Kramer, B., Mandle, L., Ziv, G., & Acuña, V. (2016). Model development for the assessment of terrestrial and aquatic habitat quality in conservation planning. *The Science of the Total Environment, 540*, 63–70. https://doi.org/10.1016/j.scitotenv.2015.03.064

Trading Economics. (2023). *United States 10 Year TIPS yield—2023 data—1997-2022 historical—2024 forecast.* Tradingeconomics.Com. https://tradingeconomics.com/united-states/10-year-tips-yield

UNFCCC. (2022). *Finance for nature-based solutions must triple by 2030.* United Nations Climate Change. https://unfccc.int/news/finance-for-nature-based-solutions-must-triple-by-2030

United Nations, Department of Economic and Social Affairs, Population Division. (2018). *Annual population of urban agglomerations with 300,000 or more in 2018 (thousands)*. World Urbanization Prospects: The 2018 Revision. https://population.un.org/wup/DataQuery/

United Nations Environment Program (UNEP). (2014). *Using models for green economy policymaking.* https://www.un-page.org/files/public/content-page/unep_models_ge_for_web.pdf

Villate Daza, D. A., Sánchez Moreno, H., Portz, L., Portantiolo Manzolli, R., Bolívar-Anillo, H. J., & Anfuso, G. (2020). Mangrove forests evolution and threats in the Caribbean Sea of Colombia. *Water, 12*(4), 1113. https://doi.org/10.3390/w12041113

Wang, M., Zhang, J., Tu, Z., Gao, X., & Wang, W. (2010). Maintenance of estuarine water quality by mangroves occurs during flood periods: A case study of a subtropical mangrove wetland. *Marine Pollution Bulletin, 60*(11), 2154–2160. https://doi.org/10.1016/j.marpolbul.2010.07.025

World Bank. (2023). *Lending rates & fees* [Text/HTML]. IBRD Financial Products. https://treasury.worldbank.org/en/about/unit/treasury/ibrd-financial-products/lending-rates-and-fees

World Economic Forum. (2022). *BiodiverCities by 2030: Transforming cities' relationship with nature*. World Economic Forum and Alexander von Humboldt Biological Resources Research Institute. https://www3.weforum.org/docs/WEF_BiodiverCities_by_2030_2022.pdf

NATURE-BASED INFRASTRUCTURE
GLOBAL RESOURCE CENTRE